Contract No.
DAAB07-68-C-0083

SCHOOL OF
ELECTRICAL ENGINEERING
OKLAHOMA STATE UNIVERSITY

A CENTER FOR THE DESCRIPTION OF ENVIRONMENTAL CONDITIONS (THEMIS PROJECT NO. 129)

WEATHER PHENOMENA

ANNUAL REPORT

TO

Department of the Army
Electronics Command

WP 69-I-4
OCTOBER 31, 1968

A Center for Description of Environmental Conditions (Themis Project No. 129) Weather Phenomena

Annual Report

Submitted to

The Department of the Army

Electronic Command

by

School of Electrical Engineering

College of Engineering

Oklahoma State University

Stillwater, Oklahoma

October 31, 1969

PREFACE

The research work described in this annual report was sponsored by the Department of Defense under Project Themis. Oklahoma State University Themis Weather Phenomena Studies are administered under contract No. DAAB07-68-C-0083.

CONTENTS

ILLUSTRATIONS

APPENDICES

I. INTRODUCTION

A. HISTORY OF PROGRAM

The College of Engineering, Oklahoma State University, submitted Proposal ER 67-T-21 entitled, "A Center for the Description of Environmental Conditions--Weather Phenomena (Themis No. 129)" to the Department of Defense on May 1, 1967, in response to the brochure, Project Themis, dated November, 1966. Authorization to implement the program, with limited funds, was given in the form of a letter contract. The effective date of the letter contract was October 1, 1967. The actual contract which authorized the initial three years of the program was signed by the contracting officer on January 16, 1968.

On January 19, 1968, a proposal for project continuation for the fourth year was submitted to the Department of Defense in response to the brochure, Project Themis, dated November, 1967. On June 11, 1968, the contract between Oklahoma State University and the Department of Defense was amended to authorize full funding for the first three years of the contract. However, no further notification of extension has been received.

B. OBJECTIVES OF PROGRAM

The proposals submitted have been based on the following objectives:

1. Immediate objective: the determination of the electromagnetic characteristics of severe weather.
2. Intermediate objective: the prediction of operationally restrictive and severe weather.
3. Long-term objective: the modification of operationally restrictive and severe weather.

C. RAT[illegible]

1. [illegible]gnition and definition of electromagnetic signature associ-

ated with specific severe weather occurances and the development of instrumentation to detect, measure, and analyze the electromagnetic energy present will provide another technique for use in short range weather forecasting. This new method, along with existing meteorological techniques, will be of benefit to the Department of Defense in tactical operations of all the services.

The modification of weather, if possible, will be of benefit to long-range military planning. The ability to either predict or cause a rainstorm, for example, in a particular area will provide a tremendous advantage in tactical operations planning.

D. IMPLEMENTATION PLANS

The program was initiated with a three-phased effort:

1. The development and use of instrumentation to measure the electromagnetic signature of certain weather phenomena (clear air turbulance, thunderstorms, tornadoes) in airborne and ground-based laboratories. (The correlation of electromagnetic data to existing meteorological information will be made on identifiable weather phenomena.)
2. The investigation of pattern recognition in the total data acquisition program (sferics, severe weather, existing meteorological information). (The mathematical modeling and information theory application to both the discrete and continuous data will attempt to provide keys for the third phase.)
3. The data analysis and application to identify indicators for probability of specific phenomena, to determine possible trigger mechanisms which induce the phenomena, and to define techniques for possible modification-abatement, diversion, or intensification of the phenomena.

4. The development of one or more simple airborne instrument packages which can be put in any aircraft for short term measurement of the severity of weather immediately ahead.

II. PROGRAM MANAGER'S SUMMARY

The program began in October of 1967 when funds became available. Equipment deliveries began in March of 1968 and were completed in July of 1968. Instrumentation and shakedown of the research aircraft were completed in August, 1968. Cooperation with the National Severe Storms Laboratory in the 1968 storm season was not possible since their data gathering program was terminated on June 1, 1968, due to the reduction of their operational funds. Cooperation with NSSL will be established in the spring of 1969 in order to obtain close correlation between meteorological data and electromagnetic signatures.

Some results with possible long-range meteorological implications have been obtained from late summer storms. These results raise questions as to the manner in which electrically charged clouds actually discharge. This, of course, is related closely to the manner in which mass flow of air, both turbulent and non-turbulent, occurs in a storm cloud. It re-emphasizes the fact that future work must now be closely correlated with meteorological data.

The details of the airborne instrumentation package are included in a later section of this report. Subject to stringent efforts to confirm some surprising results of measurements already made, these measurements indicate the following possibilities:

1. At high altitudes, cloud to cloud discharges often have much more horizontally polarized electromagnetic energy than vertically polarized energy. Cloud to ground discharges, without exception so far, have massive energies in the horizontal polarization as well as the vertical polarization when measured at high altitudes.

2. The spectral energy distribution from flash to flash (of the same total discharge) varies in essentially a non-expected manner. This implies that information on the charge distribution--and, therefore, perhaps internal mass flow patterns and cloud structure information--may well be obtained from horizontally and vertically polarized spectral distribution information. The reason is that polarization and spectral information for a particular flash are related to the discharge path length and path geometry. Thus we have our first indication that significant meteorological information (specifically on cell structure) might well be obtained from the type of measurements we are currently making.

A detailed technical paper, now under preparation, will be submitted for publication even though the results are tentative. The preceding statements, though tentative, are rather far reaching. Therefore it is necessary, in the interests of giving the reader a somewhat better understanding, to describe breifly the methods of preliminary data reduction which have led to these results. It is also necessary to describe three additional experiments which will be performed in the near future. These experiments are designed specifically to cross check these rather surprising results.

In preliminary data reduction, an analog time base expansion technique was used. Figure 1, shows the spectral distribution of successive flashes of a typical cloud to ground discharge. These energy distributions were obtained by taking horizontally and vertically polarized

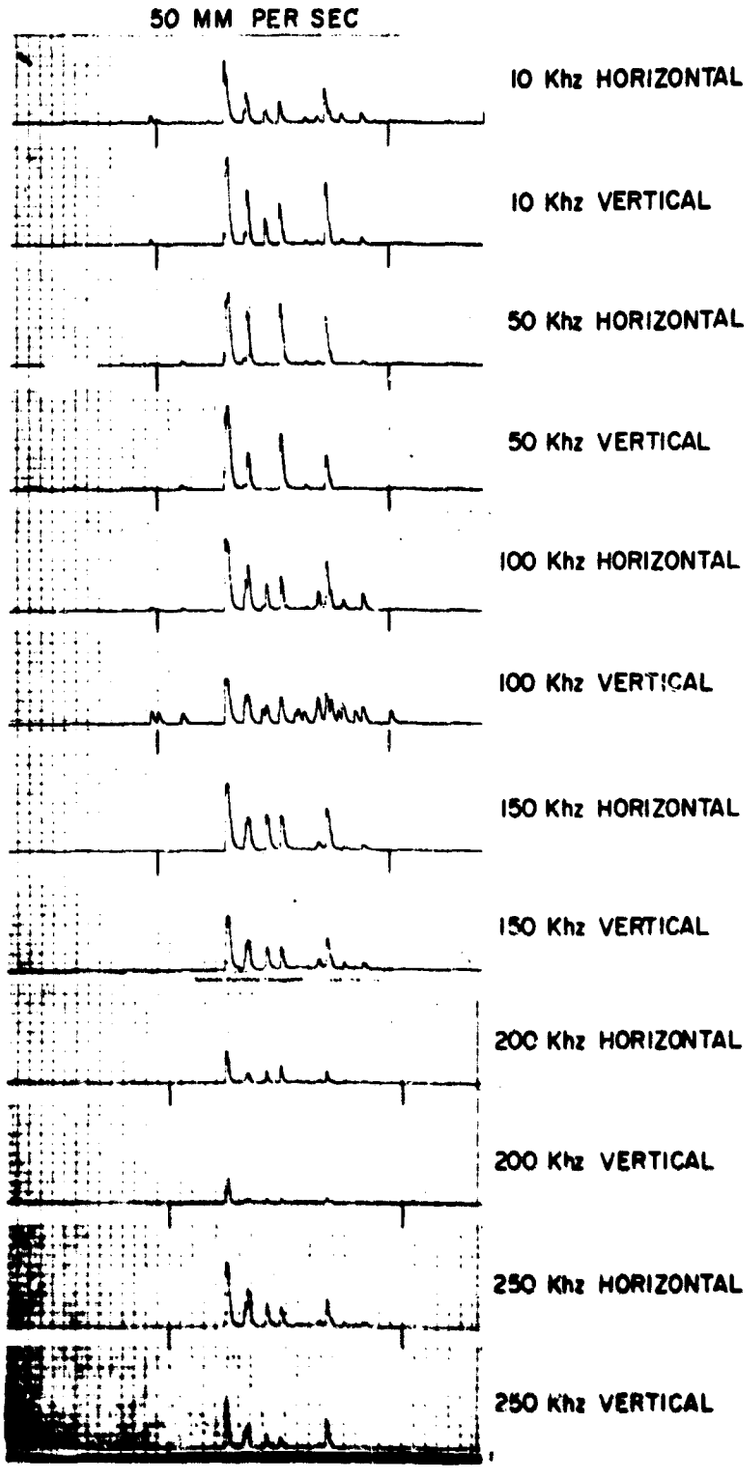

FIGURE 1. CLOUD TO GROUND DISCHARGE

comb filter outputs which were recorded on a multichannel magnetic tape recorder. The tape was time base expanded by a ratio of 4:1 and the outputs displayed on a multichannel Sanborn strip chart. The organization of the signals on the strip chart is such that 10 KHz signals of both horizontal and vertical polarization are displayed adjacent to each other, the same being true for the 50 KHz, 100 KHz, 150 KHz, 200 KHz, and 250 KHz information. While each individual flash is generally identifiable in each record, the spectral distribution and polarization energies vary widely from flash to flash, indicating different geometries. Since the visible part of the discharge indicated that each flash has the same geometry, one tentatively concludes that the intercloud flashes have radically different geometries. Records of this type will be discussed in considerable detail in forthcoming papers to be published.

Preliminary efforts are being made to select events of interest from comb filter data and then to examine wide band records of those events in fine structure detail. Time base expansion in ratios of 1000:1 have permitted us to examine both leader and return of some interesting events on an analog basis. These results, though extremely preliminary, tend to confirm the previously indicated conclusions. Within the next few months, when the digital reduction equipment discussed elsewhere in this report is installed, the time base expanded wide band signals will be fully digitized. At that point, complete energy distributions will be determined through the use of Fast Fourier transform techniques and our conclusions will be much more firm.

Several experiments, not previously anticipated, will be performed to provide scientific cross checks on this matter. These are necessary because it is not possible to be absolutely certain that the signals from each antenna have exactly the assumed polarizations. At the in-

ception of the program, it was desired to measure both polarizations to see if there were appreciable differences; however, we did not expect to find the sharp differences encountered, nor did we expect what differences we did find to have such significant meteorological implications. For these reasons, and because the program was running late due to delayed funding, placement of antennas on the aircraft was done without static model studies. We had considered reducing the antenna probes to only one after the first year. However, since that is now obviously out of the question, a model study experimental program is being set in motion to determine, as closely as possible, the amount of horizontally polarized signal being received by the vertical antenna and vice versa. Also, the aircraft will be flown to the gulf coast area or to the nearest available storm system in the near future. It will then be placed in a steep (60° or more) descending spiral from roughly an altitude of 20,000 feet to 10,000 feet with all recorders running. This violent maneuver is the only way to alter the polarization characteristics of the vertical antenna system (which unfortunately includes the airframe). It is necessary to use a descending spiral rather than a steep turn to avoid excessive G loads on the aircraft and sensitive recording equipment. It is especially important to keep such G loads down since one might encounter severe turbulence at any time near severe storms. In the spring of 1969, a special high speed camera will be set up on the ground or in a chase aircraft to make pictures of an entire isolated storm structure at approximately 250 frames per second. At the same time, the research aircraft will be measuring the storm. In this way, we hope to be able to correlate current flow patterns in the cloud (by watching where it glows) with individual cloud to ground flashes, while simultaneously recording electromagnetic signals. Thus we hope to

correlate structure with electromagnetic signatures. In these ways, we believe we can verify (or perhaps deny) our findings to date.

In addition to those experiments just discussed, the data gathering activity planned for 1969 is as follows. Beginning with the 1969 storm season, data gathering flights will be coordinated with the National Severe Storms Laboratory program in the Oklahoma area. This laboratory makes minute by minute photographic records of contour radar pictures covering about a 200 mile radius of Stillwater. This information gives good data on moisture content and severe storm centers. NSSL also gathers considerable amounts of other meteorological data in their flight and ground record programs. There is no better way to tie our electromagnetic measurements to pertinent and accurate meteorological data; thus, from about February 1 to June 1, our entire activity will be in the Oklahoma area.

For perhaps a total of ten days in July or August of 1969, we plan to make measurements at the Organ Peak Laboratory at White Sands. The opportunities for getting data of repeatable significance is perhaps greater here than anywhere else. Our aircraft will be available on Condron field for immediate flight when a storm cloud develops over Organ Peak. Storms occur on roughly thirty percent of the days during July and August. Thus, we should be able to get meaningful correlation between electromagnetic signatures and the size and state of maturity of an isolated storm for many essentially similar storms. We will simultaneously have observers on Organ Peak in communication with the aircraft so that full meteorological information is made part of the minute by minute permanent record.

One piece of equipment, a field mill, will be added to the aircraft

so that electrostatic field becomes a part of the permanent record. This addition is also believed to be necessary because the aircraft has encountered at least one condition of extreme electrostatic fields that disabled much of the other equipment. This situation is discussed elsewhere in this report.

Also, in another section of this report, a discussion is given of the digitizing equipment that will be used primarily on the wide band analog data. With this capability in full operation, it will be possible to examine in much greater detail the fine structure of the electromagnetic signature using digital Fast Fourier transform techniques. The importance of this type of analysis is becoming more obvious with the results already obtained.

The pattern recognition group has been greatly hindered by the fact that data gathering has been so far behind schedule. Their report is detailed in another section of this document. They have been making headway with the data that is now available, and have already demonstrated the digital techniques they intend to employ by using limited digitizing equipment currently available.

The cloud modeling group report is also included. This report essentially terminates that phase of the program. Our major efforts from here on are to be concentrated in the data gathering, reduction, and pattern recognition areas. This decision to shift emphasis is dictated by serious need to very closely correlate electromagnetic signatures with minute by minute meteorological data.

In summary, the achievements to date are listed as follows:

1. Design, fabrication, installation, shakedown, and operation of a sophisticated airborne instrumentation package.
2. Development and checkout of analog data reduction methods

whose application to somewhat meager data has led to interesting tentative conclusions and has called for several new experiments.

3. Development and checkout of digital reduction methods that, when combined with the use of equipment soon to be installed, will allow analysis of already discussed new phenomena in much more highly resolved detail.
4. Development and initial application of pattern recognition methods directed towards correlation of meteorological data with electromagnetic signatures, the ultimate objective of the program.

In the course of carrying out this work for the past year, many conferences have been held with other researchers in the field. Some of these are listed below.

December 18-19, 1967	Location:	White Sands Proving Grounds New Mexico
	Subject:	Instrumentation of Research Aircraft
	Participants:	Marvin Diamond - White Sands E. A. Blomerth - White Sands William L. Hughes - OSU Arthur M. Breipohl - OSU
March 8, 1968	Location:	National Center for Atmospheric Research, Boulder, Colorado
	Subject:	Electromagnetic Radiation
	Participants:	Dwayne Sarrtor - NCAR William L. Hughes - OSU Arthur M. Breipohl - OSU Victor W. Bolie - OSU
June 7, 1968	Location:	National Severe Storm Laboratory, Norman, Oklahoma
	Subject:	Coordination of NSSL and OSU Weather Research Projects
	Participants:	Edwin Kessler - NSSL Gilbert Kinzer - NSSL

		Gene Lee - NSSL William L. Hughes - OSU Arthur M. Breipohl - OSU
July 1, 1968	Location:	Oklahoma State University Stillwater, Oklahoma
	Subject:	Review Themis Weather Phenomena Program
	Participants:	Gilbert Kinzer - NSSL William L. Hughes - OSU Arthur M. Breipohl - OSU Victor W. Bolie - OSU
July 2, 1968	Location:	Oklahoma State University Stillwater, Oklahoma
	Subject:	Review Themis Weather Phenomena Program
	Participants:	W. L. Taylor - ESSA William L. Hughes - OSU Arthur M. Breipohl - OSU Victor W. Bolie - OSU
July 10, 1968	Location:	Oklahoma State University Stillwater, Oklahoma
	Subject:	Aircraft Instrumentation and Radar Equipment
	Participants:	Col. Robert W. Vincent, Air Weather Service Robert L. Overton - OSU
July 14-15, 1968	Location:	Oklahoma State University
	Subject:	Site Visit - Department of Defense Monitors
	Participants:	Themis Weather Phenomena Project Staff Frances L. Whedon - D.O.D. Wilbur Paulson - A.F. Cambridge E. A. Blomerth - White Sands R. Loveland - White Sands
August 5-9, 1968	Location:	White Sands Missile Range, New Mexico
	Subject:	Electromagnetic Radiation Data Gathering Flights in Single Cell Storms and Meetings with Atmospheric Science Laboratory Personnel.

	Participants:	William L. Hughes - OSU Gerald Stotts - OSU Keith L. Mackey - OSU Russell L. Babb - OSU Marvin Diamond - White Sands Alex Blomerth - White Sands
September 17, 1968	Location:	Institute of Atmospheric Physics
	Subject:	Discuss Themis Project Obtain Consultant for Project
	Participants:	William L. Hughes - OSU L. J. Battan - Institute of Atmospheric Physics
November 13, 1968	Location:	Oklahoma State University Stillwater, Oklahoma
	Subject:	Instrumentation of Research Aircraft
	Participants:	William L. Hughes - OSU George Kirkpatrick - University of Syracuse

A serious deficiency in the program has been the lack of on-the-spot meteorological expertise. We have hired Dr. Louis Battan as a consultant to the project and are making major efforts towards hiring a full time meteorologist. One offer was made to a highly qualified Ph.D., but after several weeks of consideration, he has declined. We are vigorously pursuing several other leads at the moment. In the meantime, Dr. Battan has exhibited considerable interest in the project and has made many helpful suggestions about the program.

The current work, during the lull in available storms, has been directed toward documenting what has already been done.

One Ph.D. thesis has resulted from the program:

1. An Analysis of Charge Transport and Equilibrium in the Global Atmosphere.

   by: Edward L. Shreve, School of Electrical Engineering.

Three technical reports have been written:

2. a. Preliminary Survey of the Present State of Knowledge of Atmospheric Electricity.

   by: Edward L. Shreve, School of Electrical Engineering.

   b. Preliminary Survey of the Present State of Knowledge on Lightning

   by: Eddy J. Milanes, School of Electrical Engineering.

   c. Preliminary Survey on the Present State of Knowledge of the Spectra From Lightning-Produced Plasma

   by: William G. Robinson, Department of Physics

One technical paper has been submitted for publication:

3. Theoretical Derivation of Atmospheric Electrical Properties

   by: Edward L. Shreve, School of Electrical Engineering

   submitted to: Journal of Geophysical Research

Four technical papers, are being written for submission for publication. Tentative titles are:

4. a. "Electric Field and Potential Around Some Thunderstorm Models"

   b. "Electromagnetic Radiation Related to Current in Lightning Discharges"

   c. "Differences Between Horizontally and Vertically Polarized Sferic Signals at High Altitudes"

   d. "Analog Method for Preliminary Reduction of Sferic Signals"

Copies of the thesis, three technical reports, and the technical paper submitted for publication are included in Appendix B (a separately bound addendum to this report).

III. DATA GATHERING

This section traces the development of the airborne data gathering assembly throughout the reporting period. Included are the results of system performance tests and the self-checks using recorded weather data. In addition, the airborne data taken during the past year is discussed in the context of system evaluation.

The test bed for the measurement apparatus is a D-18S Beechcraft airplane. Because the singular mission of the aircraft is data gathering of weather information, approval was obtained from the Federal Aviation Administration to operate in the "Restricted" category. Since the aircraft was procured in a used condition, a renovation was initiated. Concurrent with the renovation of the aircraft, provisions were made for the mounting of a vertical whip antenna atop the fuselage and a tow type antenna extending horizontally from the tail of the aircraft. A take-up or release reel has been incorporated in the horizontal antenna to facilitate the take off and landing of the aircraft. The aircraft appears as shown in Figure 2. The measurement assembly is mounted in the airplane as shown in Figure 3. The rack consists of the following commercial equipment:

1. 2 Sangamo multichannel recorders, 1 fourteen-track FM and 1 five-track wide band.
2. Hewlett-Packard oscilloscope.
3. Special Products WWV receiver.
4. Topaz power inverter.
5. American Radio Corporation transceiver.
6. Military UHF transceiver.

Additional equipment developed expressly for this project are:

1. 2 comb filter panels.

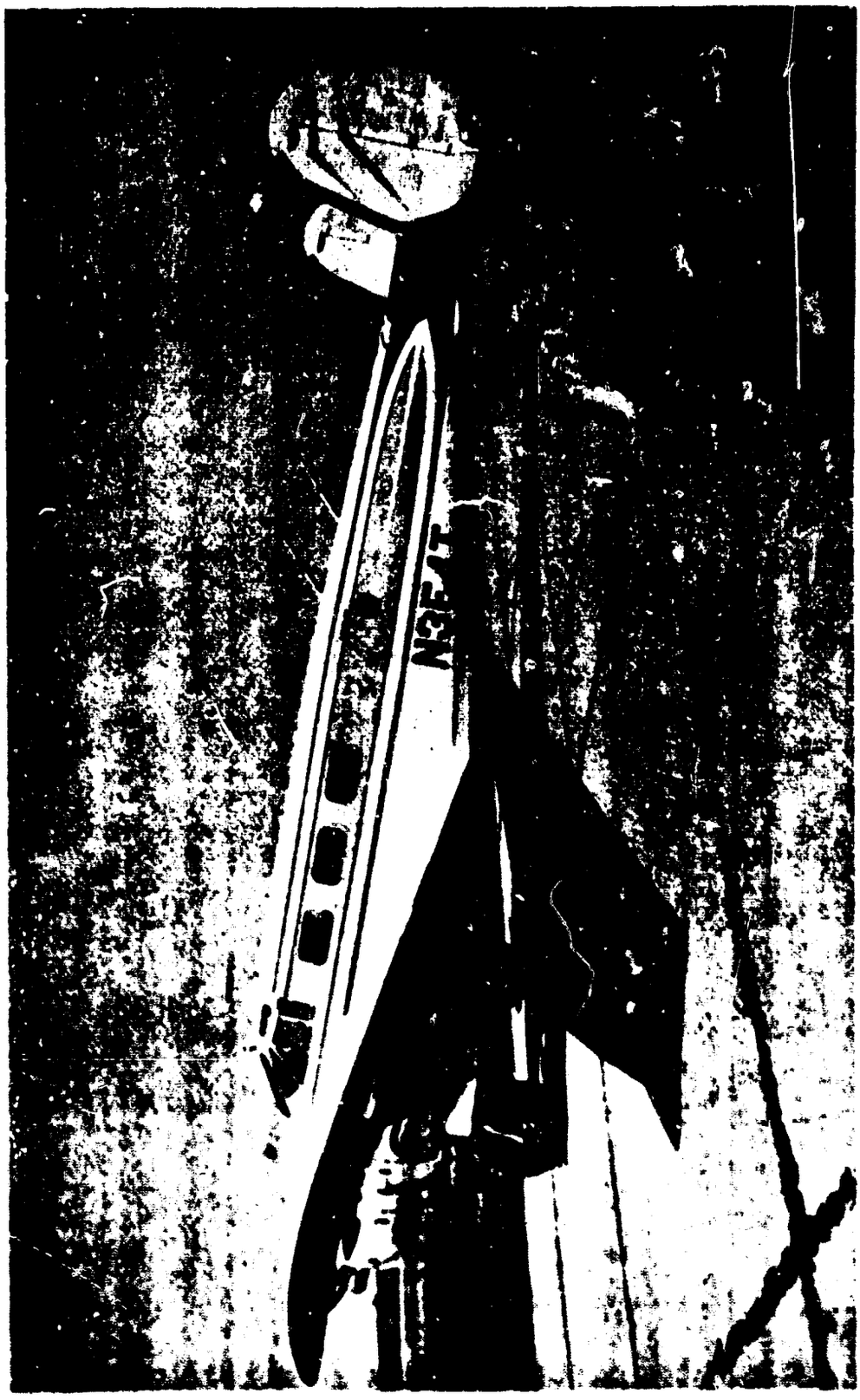

FIGURE 2. RESEARCH AIRCRAFT N354T

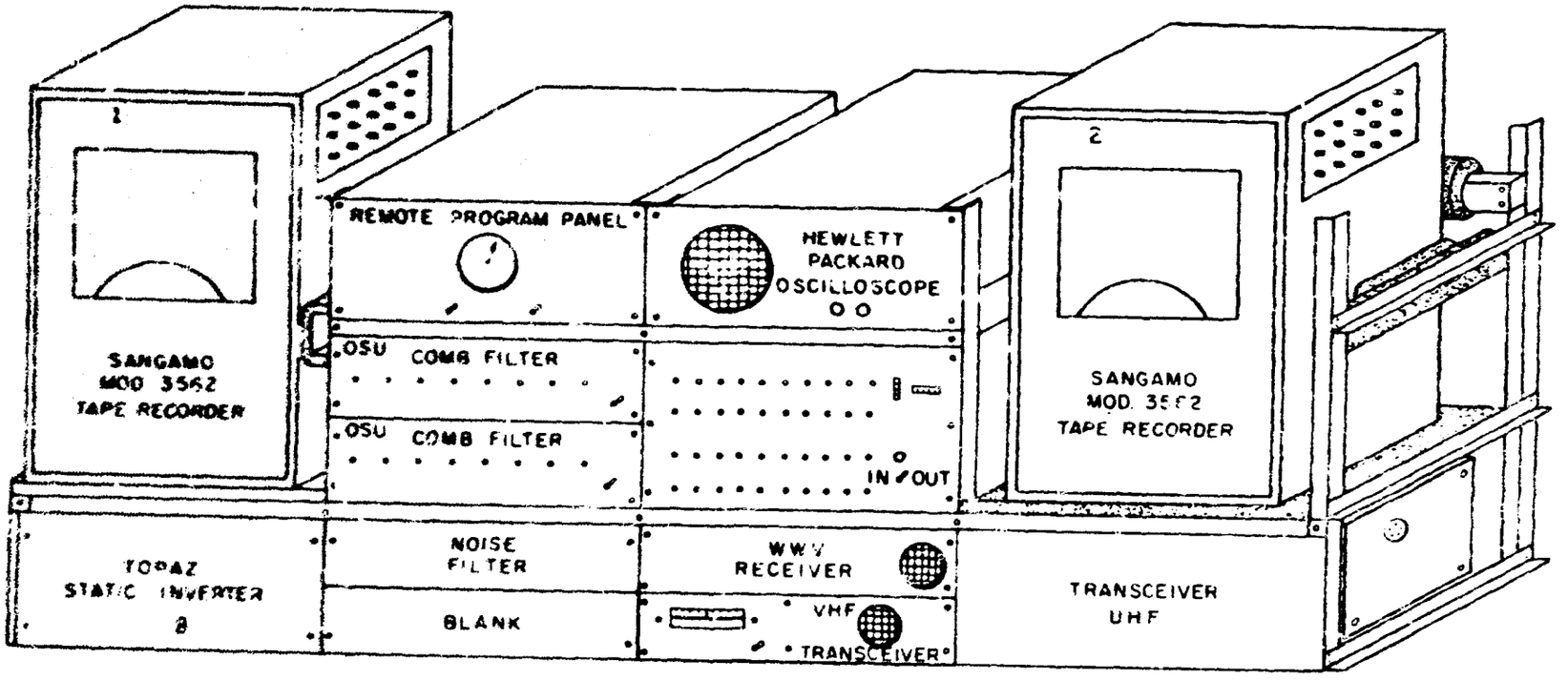

FIGURE 3. EQUIPMENT RACK - RESEARCH AIRPLANE N354T

2. Remote program panel for Sangamo 14 channel recorder.
3. DC power supply filter panel.
4. Monitor panel.

The power distribution schematic for the assembly is shown in Figure 4. All DC power is derived directly from the aircraft generation system. AC power requirements of the oscilloscope and the remote program panel are met by the use of the Topaz power inverter. In the early stages of fabrication of the data gathering assembly, tests revealed that interference from the inverter was being coupled into the aircraft DC generation system. This effect necessitated the incorporation of specially designed filters. Through the use of these filters, the interference has been sufficiently reduced.

The measurement channels are fed by the two antennas referred to earlier. This allows the simultaneous recording of vertically and horizontally polarized signals. The vertical signal flow path is shown in Figure 5. The signal gathered at the antenna is fed into a low pass filter and then through a preamp/cathode follower circuit (see Figures 6 and 7). Nuvistors are being used in this stage due to the occurrence of large transients and static charges which preclude the use of solid state devices. The low pass filter became necessary when it was discovered that grid detection of the ship's air to ground communication signal was occurring at the first cathode follower stage. The detected audio signal blanked the instrumentation during radio transmission. Because the carrier of the air-ground communication channel was well beyond the cut-off of the measurement system, it was possible to insert the low pass filter without appreciably affecting the amplitude or flatness of the desired spectrum. Due to a significant difference in signal strength between vertical and horizontal channels,

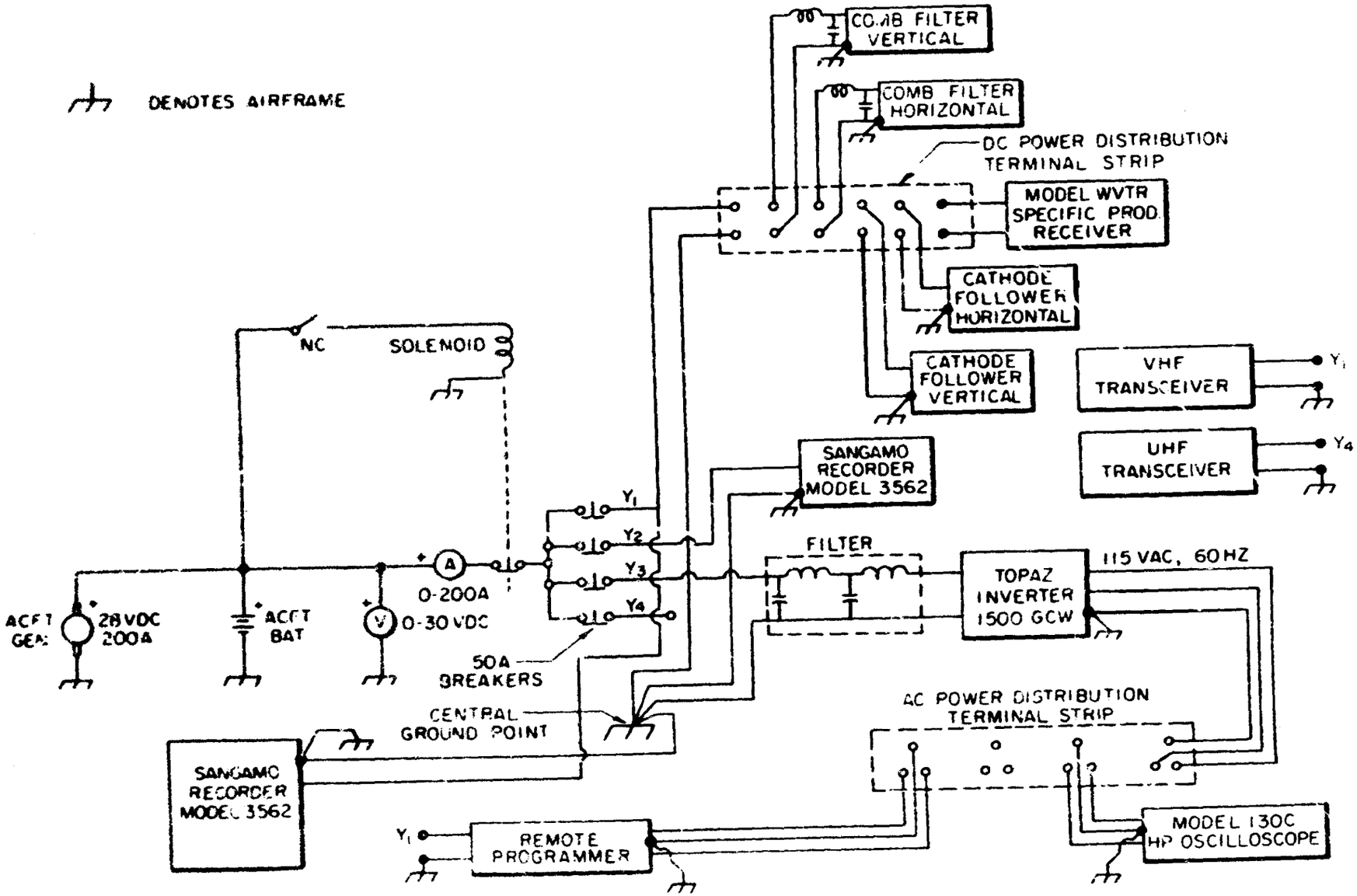

FIGURE 4 POWER DISTRIBUTION SCHEMATIC

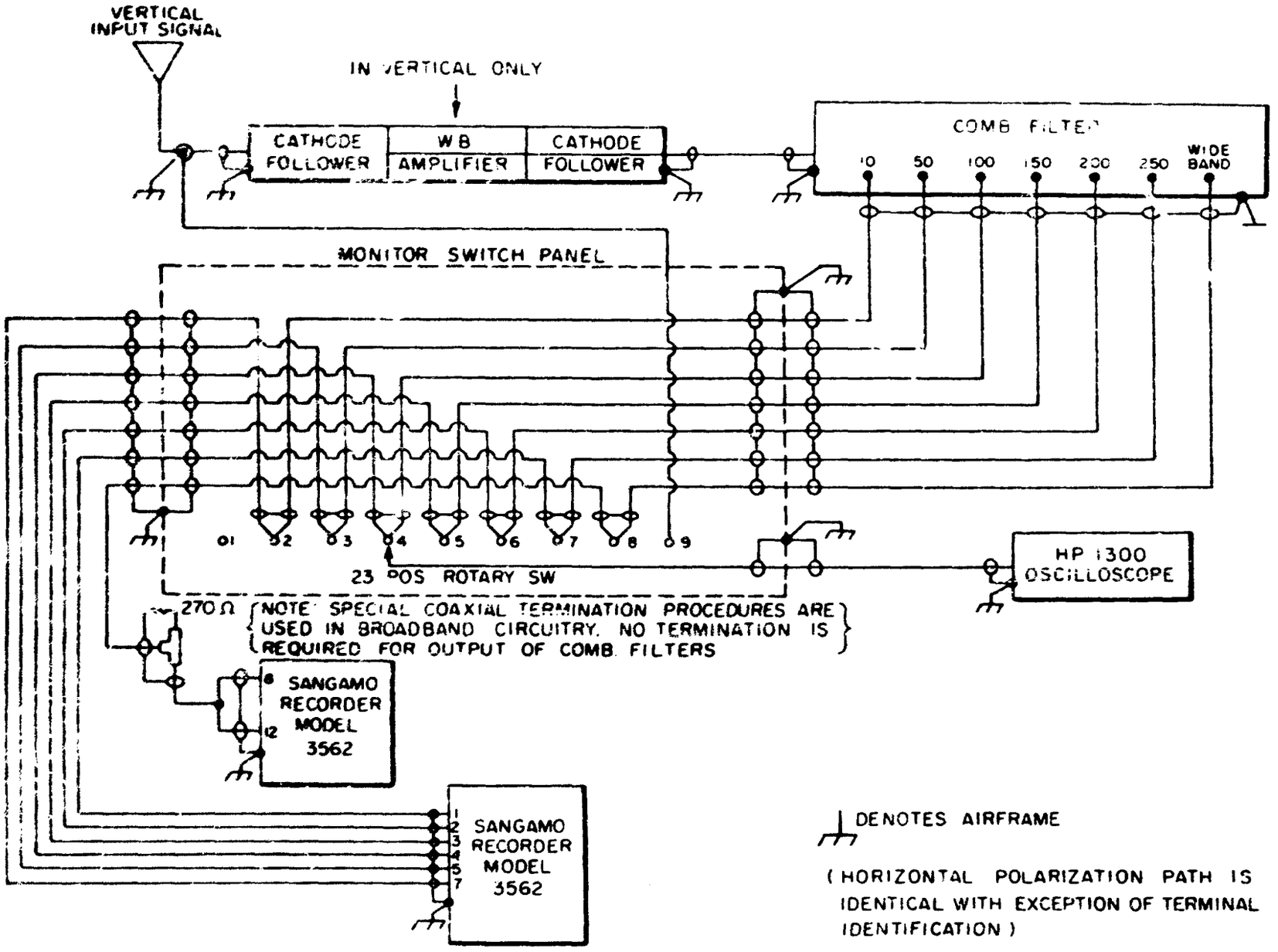

FIGURE 5 MEASUREMENT SIGNAL FLOW PATH

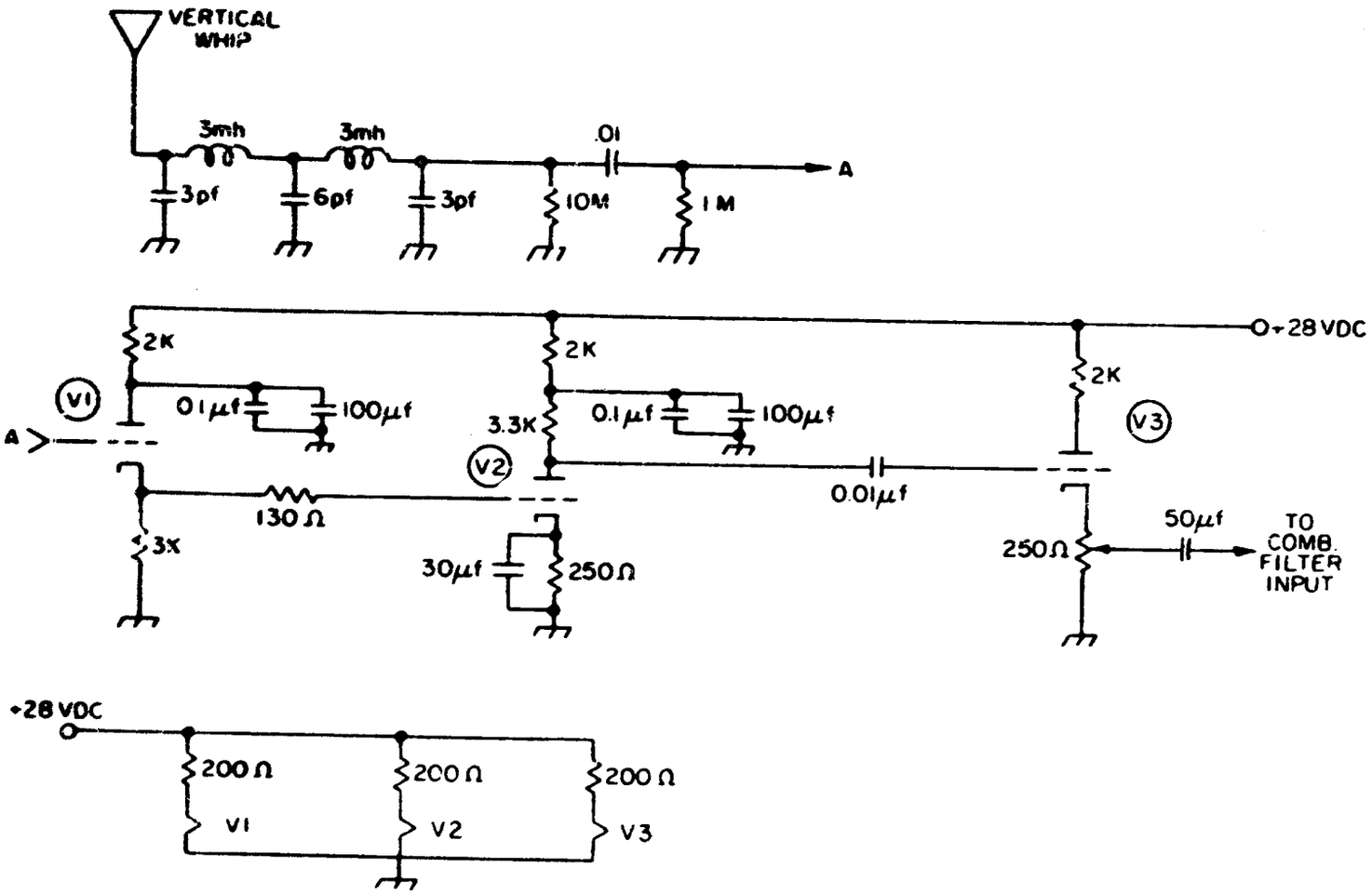

FIGURE 6 VERTICAL PREAMP/CATHODE FOLLOWER

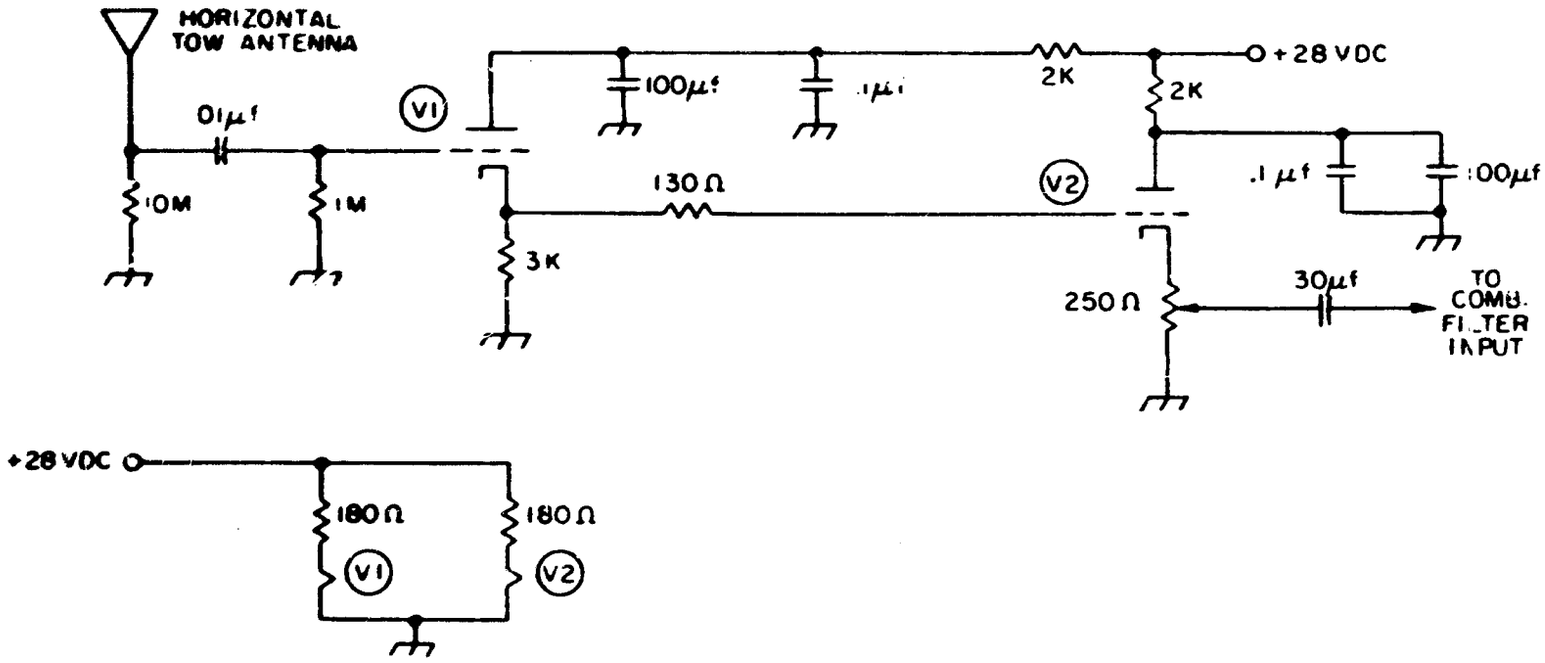

FIGURE 7 HORIZONTAL CATHODE FOLLOWER

it also became necessary to include a preamp stage in the vertical channel. This stage has a gain of about 10 dbs and raises the vertically polarized signal to the comparable range of the horizontal signal. Included in the preamp/cathode follower circuit is a two-stage cathode follower network connected in cascade. The first stage acts as a buffer to absorb high amplitude transients and static charges appearing on the antenna. Owing to the quiescent bias on the second stage, saturation of the first stage is not fed through the system. In addition, the recovery time of the system is considerably reduced.

From the preamp/cathode follower stage the signals are fed into the comb filter panel. Each comb filter panel consists of six bandpass-detector channels and one broad band channel. The circuit diagrams for typical cards of each type are shown in Figures 8 and 9. Center frequencies of the bandpass cards are 10 KHz, 50 KHz, 100 KHz, 150 KHz, 200 KHz, and 250 KHz. The pass band is 500 Hz each side of center frequency. The filtering is accomplished through the use of operational amplifiers which results in a gain of 100 over the pass band. The dynamic amplitude range of the comb filters is 0-1 millivolt peak input and 0-100 peak millivolt output. Each filter module performs an additional function, namely, envelope detection with a detection time constant of 0.001 seconds. Thus, the signal appearing at the output of each channel is the envelope of the excersions about the center frequency. The broad band channel does not have a detector system. Rather, the entire spectrum from roughly 3 KHz to 300 KHz is amplified by a factor of 30 and then recorded with no further processing.

The output of the comb filter panels is connected through the monitor panel to the recorders. The monitor panel is essentially a feed through device where the signal paths are selectively tapped by a

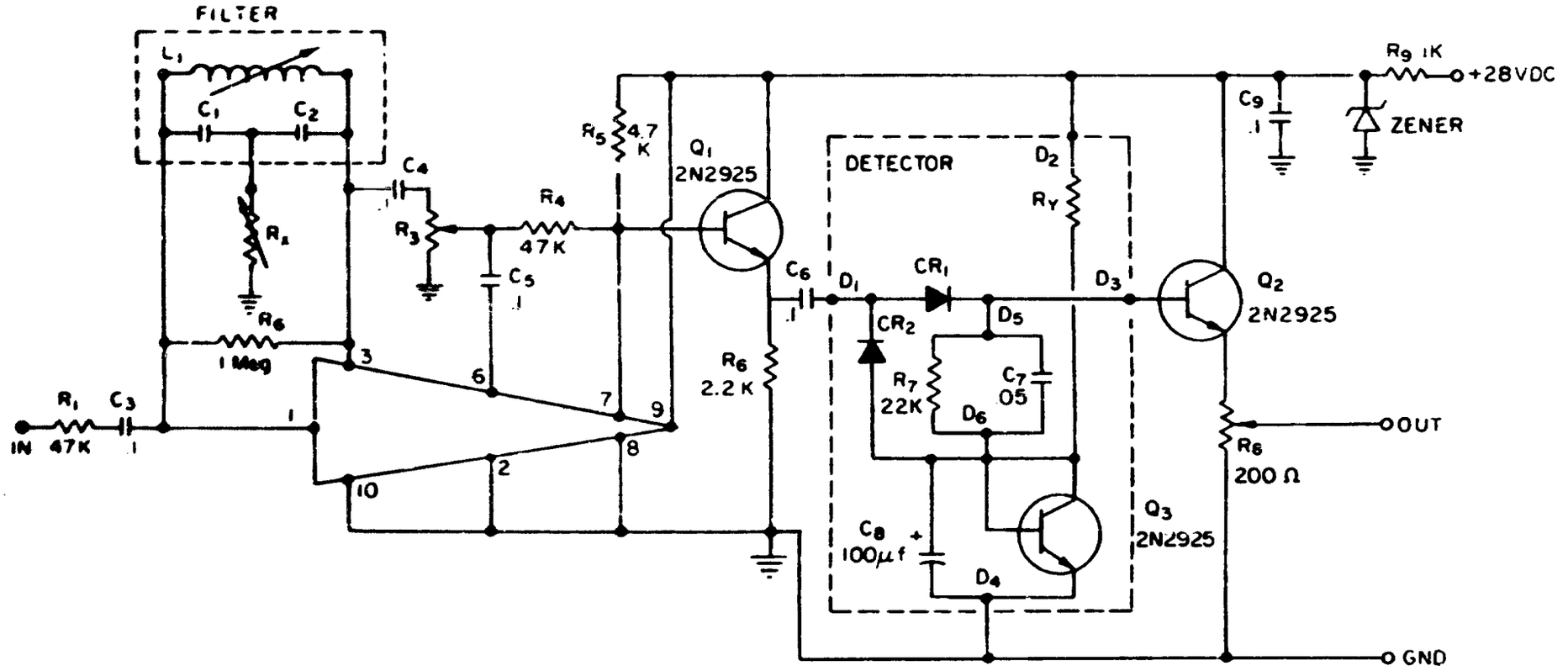

FIGURE 8 NARROW BAND AMPLIFIER

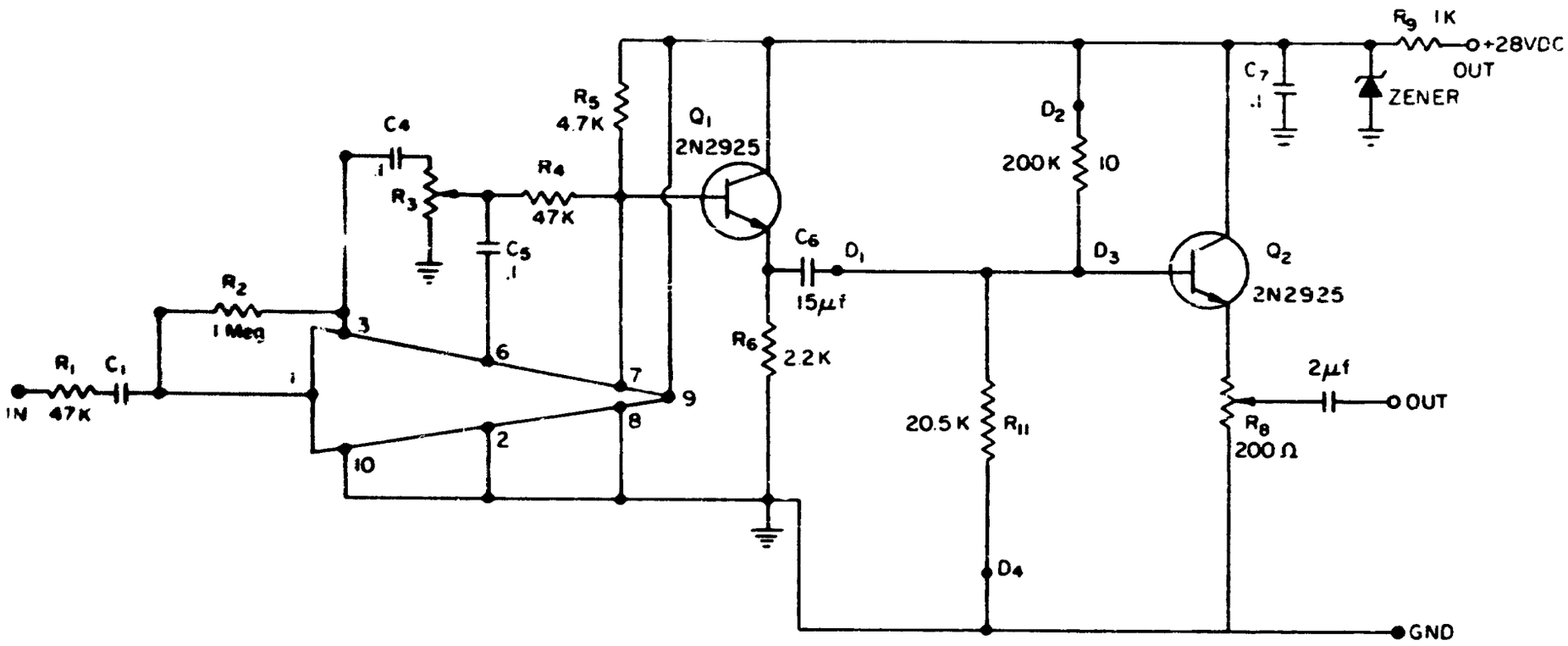

FIGURE 9. TYPICAL BROADBAND AMPLIFIER - VERTICAL AND HORIZONTAL

23 position rotary switch.

The switch wiper is connected to the oscilloscope. In addition to the comb filter outputs, a tap has been provided for the monitoring of each of the comb filter input signals. Thus, a real time display of the data before and after processing is continually available. This allows the prediction of optimal recording levels.

The detected bandpass data is recorded on 12 channels of one of the 14 channel Sangamo recorders. This recorder is equipped with FM recording modules to accommodate the low frequency characteristics of the detected data. During the data gathering mission, this recorder operates continually at a tape speed of 7 1/2 inches per second. The broad band data output of the comb filter panel is fed into 4 channels of a second Sangamo recorder. Each of the broad band outputs is recorded on an FM module and a direct module simultaneously. This recorder is operated for 1 minute every 15 minutes at a tape speed of 60 inches per second. The necessity for the parallel recording of each channel on two tracks results from the fact that the data will be recovered at 1 7/8 inches per second to gain a time base expansion. In this process, the lower frequency spectrum of the direct record module will be lost due to the frequency response of the reproducing head. However, this data will be recovered from the FM replay module. In addition to the weather data, both recorders are recording a time reference from the WWV receiver. This time reference is applied to voice edgetracks in the recorders. The recorder storing the detected outputs has a modification introduced in the edgetrack which also allows voice cueing. In addition, provisions have been made to record data from a ground station onto a second voice track contained in this recorder. The output of a VHF transceiver will be fed to this edgetrack.

The intent is to correlate the storm's electrical data with meteorological data observed from the ground or from another chase aircraft.

Because of the inconvenience experienced by the airborne technicians in the task of intermittently operating the wideband recorder, a Remote Program Panel was developed. This panel consists of an industrial timer with a cycle of 15 minutes and a variable period of actuation. Associated digital logic translates the activate period into "record" and "stop" commands to the recorder.

An additional transceiver installed in the aircraft is a UHF communicator. This was required by range safety personnel while the airplane was being operated in the vicinity of White Sands.

Following the fabrication of the measurement system and static bench tests, the assembly was subjected to airborne noise tests. The first three flights were primarily for the purpose of shaking down the system. The results of these flights resulted in several minor modifications. For example, the horizontal antenna, which is a trailing wire antenna, was found to be flapping excessively during flight. This resulted in considerable perturbations in the horizontal channel. This problem was corrected by increasing the weight of the sock at the end of the antenna. The vertical antenna was found to be picking up signals from the aircraft's air-to-ground communications equipment. The antenna was moved forward several feet to increase its distance from the communications antennas. A filter was added to the system to filter out the radio frequency signals. Later it was found the preamplifier in the horizontal channel was not required. A procedure was determined for the equalization of the gains in the two channels. This is done by equalizing the white noise levels in the wideband channels by adjusting the length of the horizontal antenna while in flight. (The horizontal antenna may be reeled in or out by the technician aboard

the aircraft merely by operating a switch on the data gathering panel.)

Flights 4 and 5 were undertaken after the system was completely operational. Flight 4 was very significant because it was the first flight in which useful data was obtained. The storm observed was a reasonably isolated cell of moderate intensity and of moderate physical size. The aircraft remained in clear air at all times during the flight. Flight 5 differed from Flight 4 in several aspects. The cells in this instance were not as well isolated as the previous flight. The cells were quite large, extending perhaps to fifty or sixty thousand feet. A large shelf extended many miles out from the cells. Much of the flying was done under this shelf. One interesting phenomena was observed while flying under this shelf. Large static charges accumulated on both the horizontal and vertical antennas. These charge accumulations and the subsequent discharges caused the comb filter inputs to saturate several times during the flight.

Because the storm season was virtually expended in the Oklahoma area, Flights 7, 8, and 9 were undertaken in the White Sands area. The data gathered during these flights are particularly valuable since the storm cells were well isolated and of moderate to high electrical intensity. In Flights 8 and 9, the visual characteristics of the electrical activity were entered on the edgetrack. The reduction of this data is currently in progress. One particularly encouraging result of this reduction was the outcome of a self-check. The broad band data was replayed through a comb filter on test bench power. The output of the filter was an exact match with the narrow band data recorded earlier in the data gathering. Hence, the repeatibility of the system holds.

In conclusion, it is felt that the data gathering assembly is completely operational and further major modifications to the existing

functional arraignment are not contemplated. The only change anticipated is to install a field mill so that static fields can be recorded.

IV. PATTERN RECOGNITION

The purpose of the pattern recognition research is to determine if the electromagnetic signature of a storm contains information which can be used to identify certain meteorological phenomenon. Pattern recognition may be accomplished by simply observing the signals recorded by the measuring instruments; however, this phase of the research is based on the assumption that there may be patterns in the received signal which can be detected only by automatic (computer) pattern recognition. With this premise, all pattern recognition efforts are based upon automatically reducing the recorded signal to a usable form for the computer.

Research to the present time has been divided into two categories, parametric and nonparametric pattern recognition. In this pattern recognition problem, the major problem is to reduce the number of measurements to a size that can be used by the computer and yet retain the significant information. In the parametric pattern recognition, we hope to select measurements that seem reasonable and let the computer determine if the selected measurements are sufficient to predict meteorological phenomenon.

The following sections describe these two phases of this research.

A. PARAMETRIC PATTERN RECOGNITION

In this phase of the project, a model, based on the sferic measurements, is being derived to hopefully aid in the classification of a given storm. There is no intention to model exactly the electromagnetic phenomena occurring within the storm. What is desired is a model that will represent the average effect of these phenomena in such a manner that it may be used successfully in a pattern classification process. The procedure being followed to derive this model

may be summarized as follows:

1. Obtain a basic model for a general sferic generating discharge.
2. Relate this model to observations at the antenna.
3. Use the sferic measurements at the antenna to improve the model.
4. Ultimately use the refined model to classify storms.

At this point, a basic model has been assumed that consists of an electric and a magnetic dipole. These dipoles have been related to the sferics measured at the antenna through conventional electromagnetic field calculations. Sferic recordings obtained on past storms are now being used to determine the form of the improved model. The results obtained under each of the outlined steps in the procedure will be discussed in the following four sections, respectively.

Basic Model

An exact model of the individual electrical activities occurring within the storm will not be attempted. For example, lightning strokes obviously contribute to the measured sferics; however, lightning strokes will not be modeled as such. One reason for this approach is the difficulty in modeling due to the randomness associated with the paths, times of occurrence, waveforms, and branching conditions of the strokes. However, most important is the possibility that the formulation of a model in terms of lightning strokes and other familiar discharges may neglect some type of discharge that is not familiar but contributes to the sferic measurements and contains information invaluable for storm classification. Thus, rather than requiring the basic model to represent several particular electrical phenomena within the storm, it is required that the basic model represent a general sferic generating element. An electric dipole and a magnetic dipole have been chosen to represent this element. Later in the procedure,

several of these dipoles will be combined into an improved model such that the sferics generated by this improved model will agree with the sferics measured.

The assumption of dipoles for the basic model may seem somewhat over simplified. However, as stated earlier, it is not desired to obtain an exact model of the actual discharges which are occurring. It is intended to formulate a model which represents, on the average, the sferics as measured by the antenna so that a pattern classification process may be applied. Since the mechanisms which generate a particular sferic are not unique, the model may be as flexible as desired as long as the sferics it generates correspond to the measurements at the antenna.

The remainder of this section will be devoted to describing the form in which the electric dipole is to be used in the basic model. The notation for the magnetic dipole will not be discussed other than noting that it has a form identical to the electric dipole with the subscripts changed from e to m on all variables and parameters.

In reference to Figure 10, the dipole is assumed to be located at the random point (X_e, Y_e, Z_e) with orientation (l_e, m_e, n_e). The observer is located at the point (x, y, z). Since the sferics are not expected to occur at fixed intervals of time, neither should radiation from the dipole occur in this manner. Thus, it is assumed that the dipole will begin radiation at the random times T_i with current waveforms $\omega_i(t)$. The current expression for the dipole becomes

$$j(t) = \sum_{i=-\infty}^{\infty} \omega_i(t - T_i)$$

This process is commonly known as "shot noise".

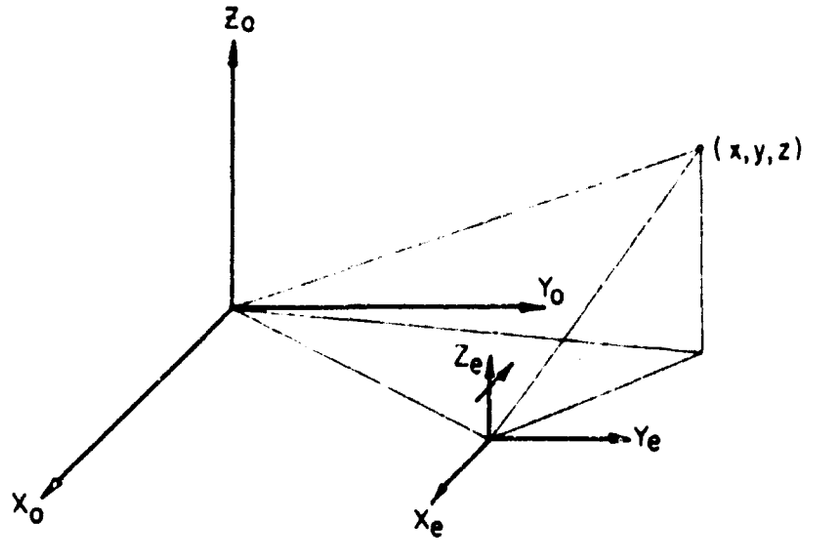

Figure 10. COORDINATE SYSTEM

The basic model explicitly involves the orientation parameters l_e, m_e, n_e which must be learned. In addition to these, the form of the distribution functions must be derived for the assumed random point of occurrence in space and time. These distribution functions will undoubtedly contain additional parameters which must be learned. Also, it is assumed that the waveform $\omega_i(t)$ is time harmonic and may be expressed in a Fourier series which introduces more parameters in terms of the Fourier coefficients.

The learning of these distributions along with all parameters introduced will be accomplished through the sferic measurements at the antenna. This is the topic for discussion in section I-C.

Before the antenna data is used to learn the distributions and parameters of the basic model and to expand this model, the radiation from the basic model must be calculated so that it is related to the antenna. These calculations will be discussed in the following section.

Field Calculations

The electric dipole may be represented by a positive time varying charge, Q(t), separated from an equal but opposite polarity charge -Q(t), by a distance ΔL along the unit vector (l_e, m_e, n_e). (See Figure 11.) Mathematically, the dipole may be expressed by the polarization vector

$$\vec{P}(t) = Q(t)\, \Delta L\, \vec{a}_e ,$$

where a_e is the unit vector (l_e, m_e, n_e).

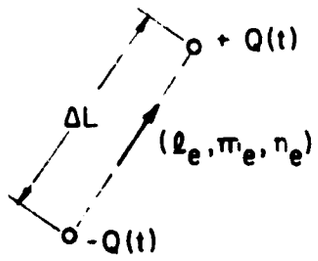

Figure 11. DIPOLE REPRESENTATION

The field distribution will be calculated by determining the Hertz vector at the observation point (x, y, z). The Hertz vector resulting from the above polarization vector located at the point (x', y', z') is given by

$$\vec{\Pi}(x, y, z, t) = \frac{1}{4\pi\varepsilon_o} \int \vec{P}(x', y', z', t - r/v)\, \frac{1}{r}\, dv' ,$$

where r is the distance $[(x - x')^2 + (y - y')^2 + (z - z')^2]^{1/2}$ and v is the propagation velocity of the wave. In these calculations, ΔL will be chosen such that the Hertz vector may be approximated as

$$\vec{\Pi}(x, y, z, t) \doteq \frac{1}{4\pi\varepsilon_o r} \vec{P}(t - r/v) ,$$

or

$$\vec{\Pi}(x, y, z, t) \doteq \frac{1}{4\pi\varepsilon_o r} Q(t - r/v)\, \Delta L \vec{a}_e \ .$$

The field conditions are given in terms of the Hertz vector by the equations

$$\vec{E} = \nabla(\nabla \cdot \vec{\Pi}) - \mu\varepsilon \frac{\partial^2 \vec{\Pi}}{\partial t^2} \ ,$$

and

$$\vec{B} = \mu\varepsilon\, \nabla \times \frac{\partial \vec{\Pi}}{\partial t} \ .$$

Assuming the dipole is time harmonic, the above two equations become

$$\vec{E} = \nabla(\nabla \cdot \vec{\Pi}) + \mu\varepsilon\omega^2 \vec{\Pi}$$

and

$$\vec{B} = j\omega\mu\varepsilon\, \nabla \times \vec{\Pi} \ .$$

Before continuing with the procedure, two reasons for using the Hertz vector approach to the field calculations will be noted. First, the dipole current distribution is given by $J = \partial P/\partial t$. Thus, rather than requiring the current distribution to be known, the chosen formulation needs only its time average. Second, the field conditions for the magnetic dipole may be obtained with ease from the field conditions of the electric dipole. This will be discussed at the end of the section.

In determining the field conditions from the equations for E and H the calculations will not be limited to the far field. Kraus [1][1] states

---

[1] References cited are shown in Appendix A.

that the boundary between the near and far fields for a dipole antenna may be taken to be at a radius $R = 2L^2/\lambda$, where L is the length of the antenna and λ is the wavelength of the radiation frequency. If the model were required to represent a cloud to ground stroke one mile in height, a sample R may be calculated using the frequencies of 10 KH. and 250 KH., which are the extremes of the narrow band recordings. These frequencies yield R = 0.43 miles for 10 KH. and R = 10.7 miles for 250 KH. Thus, at the higher frequencies we are not guaranteed far field conditions, and the calculations must include all components of the field.

To account for the boundary conditions at the earth's surface, image theory is assumed to hold. Under this assumption, the effect of the earth's surface may be represented by the original dipole's image. This consists of a dipole identical to the original dipole and located a distance of 2h directly below the original dipole with orientation $(-l_e, -m_e, n_e)$. Here it is assumed that the original dipole was located at a height h above the earth's surface. The wave guide effect produced by the earth's surface and the ionosphere, and the ground wave effect have briefly been investigated and believed to be negligible. Thus, the problem of calculating the radiation from an electric dipole located a height h above the earth's surface will be approximated by calculating the radiation from the original dipole and its image in free space.

For the present calculation, the dipole will be located at the point (o, o, h) and its image at (o, o, -h); the observer is at (x, y, z). The Hertz vector at the observation point is given by

$$\left(\frac{4\pi\epsilon_o}{\Delta L}\right)\vec{\Pi} = \vec{a}_x\, l_e \left(\frac{Q_1}{r_1} - \frac{Q_2}{r_2}\right) + \vec{a}_y\, m_e \left(\frac{Q_1}{r_1} - \frac{Q_2}{r_2}\right) + \vec{a}_z\, n_e \left(\frac{Q_1}{r_1} + \frac{Q_2}{r_2}\right),$$

where $\vec{a}_x$, $\vec{a}_y$, and $\vec{a}_z$ are unit vectors in the x, y, and z directions, respectively;

$$r_1 = [x^2 + y^2 + (x - h)^2]^{1/2} ,$$

$$r_2 = [x^2 + y^2 + (x + h)^2]^{1/2} ,$$

$$Q_1 = Q(t - r_1/v) ,$$

and

$$Q_2 = Q(t - r_2/v) .$$

The above Hertz vector has been converted to spherical coordinates and the field calculated from the equations for $\vec{E}$ and $\vec{B}$. These results will be given in terms of their spherical components E_r, E_θ, E_ϕ, B_r, B_θ, and B_ϕ where $\vec{E} = E_r\vec{a}_r + E_\theta\vec{a}_\theta + E_\phi\vec{a}_\phi$ and $\vec{B} = B_r\vec{a}_r + B_\theta\vec{a}_\theta + B_\phi\vec{a}_\phi$.

$$E_r = \frac{\Delta L}{4\pi\epsilon_o} \{\sin\theta(\ell\cos\phi + m\sin\phi)[-Q_{1,2}(2, 3; -2, -3) + \mu\epsilon\omega^2 Q_{1,2}(1; -1)]$$

$$+ n\cos\theta[-Q_{1,2}(2, 3; 2, 3) + \mu\epsilon\omega^2 Q_{1,2}(1; 1)]$$

$$+ Q_1(3, 4, 5)(r - h\cos\theta)[r n\cos\theta - hn + r\sin\theta(\ell\cos\phi + m\sin\phi)]$$

$$+ Q_2(3, 4, 5)(r + h\cos\theta)[r n\cos\theta + hn - r\sin\theta(\ell\cos\phi + m\sin\phi)]\}.$$

$$E_\theta = \frac{\Delta L}{4\pi\epsilon_o} \{\cos\theta(\ell\cos\phi + m\sin\phi)[-Q_{1,2}(2, 3; -2, -3) + \mu\epsilon\omega^2 Q_{1,2}(1; -1)]$$

$$+ n\sin\theta[Q_{1,2}(2, 3; 2, 3) - \mu\epsilon\omega^2 Q_{1,2}(1; 1)]$$

$$- h\sin\theta[hn - r\sin\theta(\ell\cos\phi + m\sin\phi)][Q_1(3, 4, 5) + Q_2(3, 4, 5)]$$

$$+ hnr\sin\theta\cos\theta[Q_1(3, 4, 5) - Q_2(3, 4, 5)]\} .$$

$$E_\phi = \frac{\Delta L}{4\pi\varepsilon_o}\{(\ell \sin\phi - m\cos\phi)[Q_{1,2}(2, 3; -2, -3) - \mu\varepsilon\omega^2 Q_{1,2}(1; -1)]\} .$$

$$E_r = \frac{\Delta L}{4\pi\varepsilon_o}(j\omega\mu\varepsilon)\, h \sin\theta(\ell \sin\phi - m\cos\phi)\, Q_{1,2}(2, 3; 2, 3) .$$

$$E_\theta = \frac{\Delta L}{4\pi\varepsilon_o}(j\omega\mu\varepsilon)(-\ell \sin\phi + m\cos\phi)[r\, Q_{1,2}(2, 3; -2, -3) - h\cos\theta\, Q_{1,2}(2, 3; 2,3)].$$

$$H_\phi = \frac{\Delta L}{4\pi\varepsilon_o}(j\omega\varepsilon)\{Q_{1,2}(2, 3; 2, 3)[rn \sin\theta + h(\ell\cos\phi + m\sin\phi)]$$

$$- Q_{1,2}(2, 3; -2, -3)\, r\cos\theta(\ell\cos\phi + m\sin\phi)\} .$$

Where

$$Q_{1,2}(1; \pm 1) \triangleq \frac{Q_1}{r_1} \pm \frac{Q_2}{r_2} .$$

$$Q_i(3, 4, 5) \triangleq -\left(\frac{\omega}{v}\right)^2 \frac{Q_i}{r_i^3} + j3\left(\frac{\omega}{v}\right)\frac{Q_i}{r_i^4} + 3\frac{Q_i}{r_i^5}, \quad i = 1,2 .$$

$$Q_{1,2}(2, 3; \pm 2, \pm 3) \triangleq j\left(\frac{\omega}{v}\right)\frac{Q_1}{r_1^2} + \frac{Q_1}{r_1^3} \pm j\left(\frac{\omega}{v}\right)\frac{Q_2}{r_2^2} \pm \frac{Q_2}{r_2^3} .$$

In addition to these calculations, the following has been performed as a check on these results. A Hertz vector was defined for the original dipole in terms of a spherical coordinate system which had the dipole at its origin, and the field conditions were calculated. The same was performed for the image dipole and its coordinate system. The two fields were superimposed and converted to the coordinate system used in the first calculations, and the results were found to agree with those given above.

In the event that it is desired to have the field conditions expressed in terms of a spherical coordinate system translated in the xy-plane, the following result is needed. For example, see Figure 10

in the first section. Here the (x, y, z) coordinates are translated by the vector (x_e, y_e, o) with respect to the $x_o, y_o, z_o)$ coordinate system. That is $(x_o, y_o, z_o) = (x + x_e, y + y_e, z)$. The transformation of a vector $\vec{A} = \vec{a}_r A_r + \vec{a}_\theta A_\theta + \vec{a}_\phi A_\phi$ into a vector $\vec{A} = \vec{a}_{r_o} A_{r_o}$ $+ \vec{a}_{\theta_o} A_{\theta_o} + \vec{a}_{\phi_o} A_{\phi_o}$ is given by

$$A_{r_o} = A_r\{(\sin\theta\cos\theta)\sin\theta_o\cos\phi_o + (\sin\theta\sin\phi)\sin\theta_o\sin\phi_o + (\cos\theta)\cos\theta_o\}$$

$$+ A_\theta\{(\cos\theta\cos\phi)\sin\theta_o\cos\phi_o + (\cos\theta\sin\phi)\sin\theta_o\sin\phi_o - (\sin\theta)\cos\theta_o\}$$

$$+ A_\phi\{-(\sin\phi)\sin\theta_o\cos\phi_o + (\cos\phi)\sin\theta_o\sin\phi_o\},$$

$$A_{\theta_o} = A_r\{(\sin\theta\cos\phi)\cos\theta_o\cos\phi_o + (\sin\theta\sin\phi)\cos\theta_o\sin\phi_o - (\cos\theta)\sin\theta_o\}$$

$$+ A_\theta\{(\cos\theta\cos\phi)\cos\theta_o\cos\phi_o + (\cos\theta\sin\phi)\cos\theta_o\sin\phi_o + (\sin\theta)\sin\theta_o\}$$

$$+ A_\phi\{(-\sin\phi)\cos\theta_o\cos\phi_o + (\cos\phi)\cos\theta_o\sin\phi_o\},$$

and

$$A_{\phi_o} = A_r\{-(\sin\theta\cos\phi)\sin\phi_o + (\sin\theta\sin\phi)\cos\phi_o\}$$

$$+ A_\theta\{-(\cos\theta\cos\phi)\sin\phi_o + (\cos\theta\sin\phi)\cos\phi_o\}$$

$$+ A_\phi\{(\sin\phi)\sin\phi_o + (\cos\phi)\cos\phi_o\},$$

where

$$\cos\theta = \frac{r_o}{r}\cos\theta_o,$$

$$\sin\theta = \{1 - (\frac{r_o}{r})^2\cos^2\theta_o\}^{1/2},$$

$$\sin\phi = (r_o\sin\theta_o\sin\phi_o - y_e) / (r^2 - r_o^2\cos^2\theta_o)^{1/2},$$

and

$$\cos\phi = (r_o\sin\theta_o\cos\phi_o - x_e) / (r^2 - r_o^2\cos^2\theta_o)^{1/2}.$$

As in the electric dipole calculations, the field due to a magnetic dipole above the earth's surface may be calculated by considering the actual dipole and its image radiating in free space. Thus, according to the principle of complementary solutions, the field expressions for the magnetic dipoles may be obtained from those of the electric dipole by the relations

$$\vec{E}' = -\sqrt{1/\mu\epsilon}\ \vec{B},$$

and

$$\vec{B}' = \sqrt{\mu\epsilon}\ \vec{E}\ .$$

There is only one additional point to note. For an electric dipole with orientation (l_e, m_e, n_e), the image will have orientation $(-l_e, -m_e, n_e)$, but for a magnetic dipole with orientation (l_m, m_m, n_m), its image, due to an assumed infinite conducting plane, will have orientation $(l_m, m_m, -n_m)$. Thus, in the above expressions replace l by -l, m by -m, and n by -n when these are associated with the r_2 terms.

Model Improvement

The basic model related to the antenna still contains all of the unknowns it originally had at formulation:

1. The time distribution and its associated parameters.
2. The space distribution and its parameters.
3. The orientation parameters.
4. The Fourier coefficients of the waveform.
5. The number of elements and their positions required to build up the "improved model".

It is suspected that the fifth unknown will be strongly affected by the first four, or possibly absorbed into them.

The work to be done in model improvement consists of using the

antenna data to learn the unknowns listed above. These unknowns contain the parameters of parametric pattern recognition. At this point only the first of the five has been considered in any detail. The remainder of this section will be devoted to results obtained that concern this time distribution.

The data used to investigate the time distribution was obtained from an isolated cell in New Mexico. Only the sferic bursts which correspond to visually confirmed lightning strokes have been utilized at the present time. Except for a very few strokes which seemed to trigger several succeeding strokes, the data appeared to satisfy the basic postulates of a Poisson process. Thus the Poisson process was chosen as a likely candidate.

The distribution function, $F_T(t)$, for the time between strokes, may be obtained as follows:

$$P(T > t) = \text{Prob. [no strokes in the interval } (o, T)]$$

$$= e^{-\lambda t} .$$

$$F_T(t) = P(T \leq t) = 1 - P(T \geq t) = 1 - e^{-\lambda t} .$$

The above equation may be rearranged to yield

$$-\lambda t = \ell n[1 - F_T(t)] .$$

A magnitude scaled sample distribution, $F_T^S(t)$, has been obtained from the data. The scale factor is 214 since there were 214 observations. Thus if

$$F_T^S(t) = 214(1 - e^{-\lambda t}) ,$$

then

$$-\lambda t = - \ln 214 + \ln(214 - F_T^S(t)) ,$$

and a plot of $(214 - F_T^S(t)$ verses t on semi-logarithmic paper should yield a straight line with slope $-\lambda$. These results are shown for $\lambda = .0682$ in Figure 12. Figure 13 shows $F_T^S(t)$ verses t in dots and the function $214(1 - e^{-.0682t})$ as a continuous line. From these graphs, it appears that the function $F_T(t) = 1 - e^{-.0682t}$ is a reasonable estimate for the distribution function of this particular storm.

Consider now the corresponding density function

$$f_T(t) = \frac{dF_T(t)}{dt} = \lambda e^{-\lambda t} .$$

For the assumed value $\lambda = .0682$, the scaled density function is

$$f_T^S(t) = 214\ \lambda e^{-\lambda t} = 14.6\ e^{-.0682t} .$$

This function is compared with the empirical density function $f_T^S(t)$ in Figure 14 of this section. Consideration of the empirical density function suggests that it may be other than Poisson with uniform λ. One form suggested by the shape of the empirical function is a Rayleigh distribution. However, this is in total disagreement with the sample distribution. Another possibility is that the rate is Poisson distributed, but λ is not constant.

This summarizes the work done to present. The following section will mention briefly the intended method of classification of the storm and the "criterion of goodness" for the model.

Pattern Recognition

How the model is to be used in classification can not be exactly specified until further work is done. It may be possible to classify a storm by considering only changes in the model's parameters, or the model may require a change in form as the storm progresses. In any event, it is claimed for the purposes of this phase that any model which yields

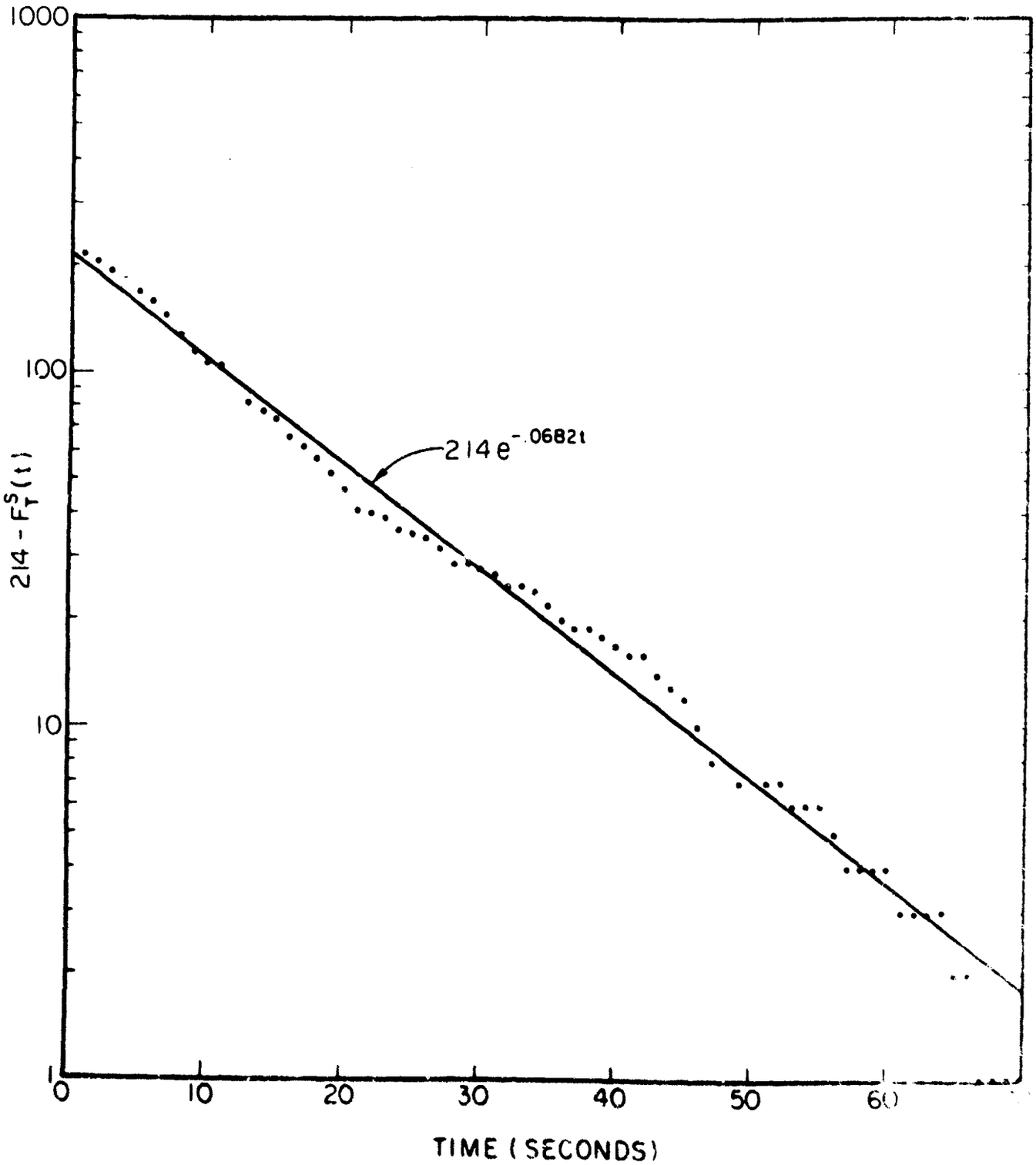

FIGURE 12 LOG $[214 - F_T^S(t)]$ VERSUS TIME

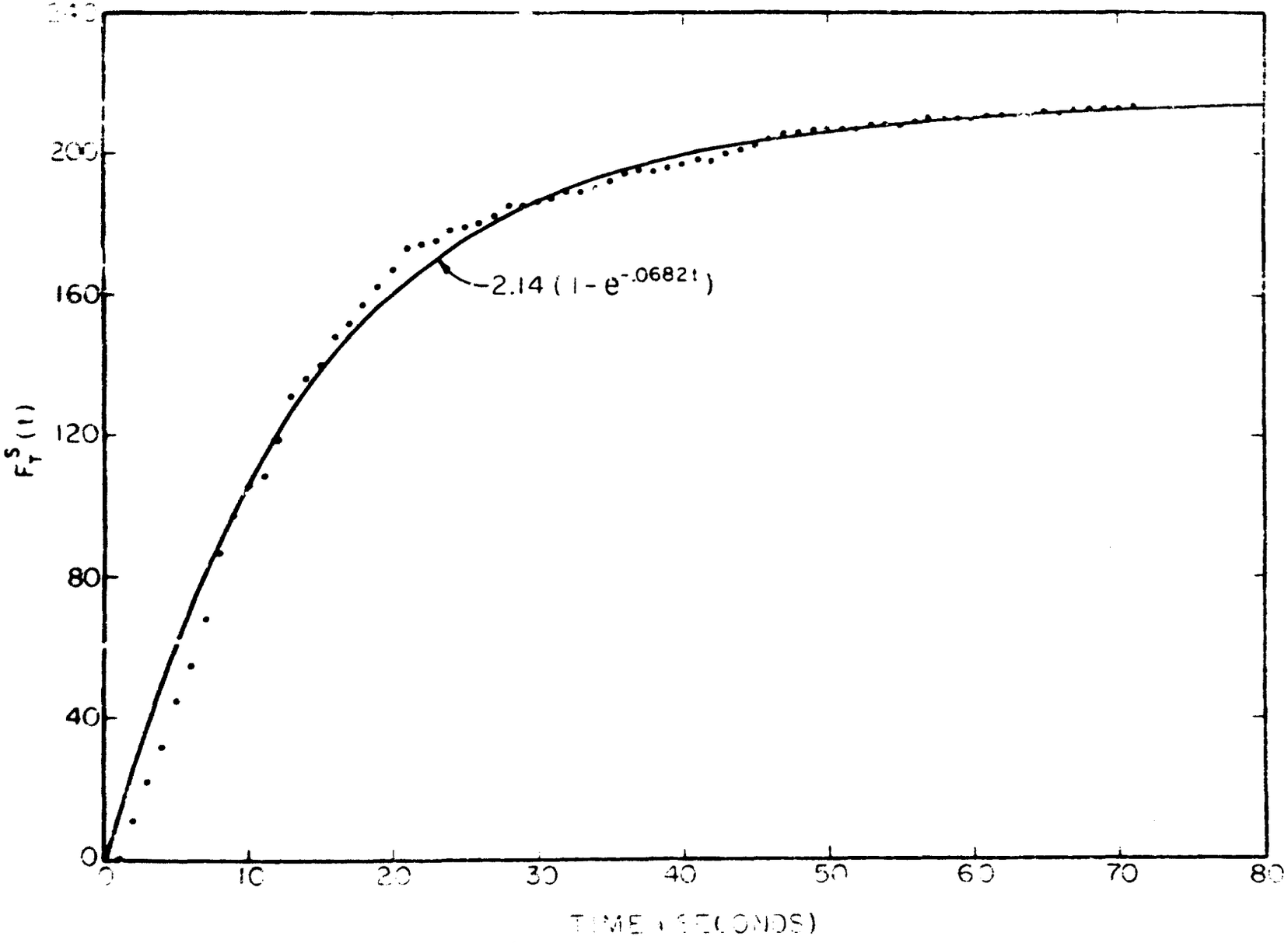

FIGURE 3 $F_T^S(t)$ VERSUS TIME

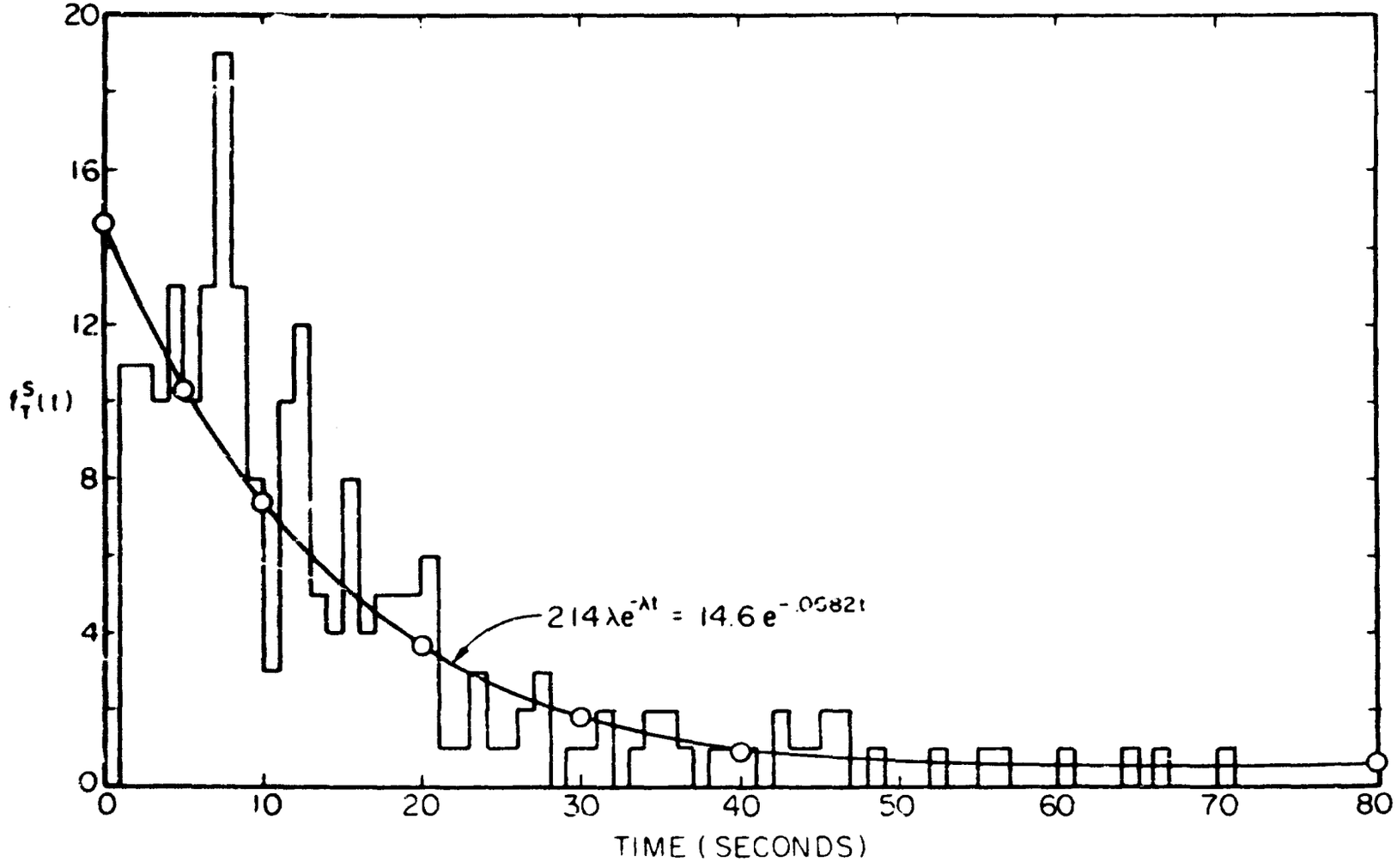

FIGURE 14 $f_T^S(t)$ VERSUS TIME

a "noticeable" difference as the storm changes will be a "good" model.

B. NONPARAMETRIC PATTERN RECOGNITION

Introduction

Two nonparametric methods of pattern recognition, threshold logic, and nearest neighbor rules have been investigated and programmed on the computer. These methods are described briefly in following sections. Both of these methods require changing the form of the recorded data to the form required by the computer (data reduction) and selecting from the many possible measurements those that are to be used (measurement selection) in pattern recognition.

Although the ultimate goal of pattern recognition is to identify meteorological phenomenon, an intermediate project is to classify lightning discharges into two categories: Cloud to cloud and cloud to ground. This project was selected in order to test the pattern recognition programs with presently available data.

Threshold Logic Unit

The threshold logic unit (TLC) is a linear trainable pattern classifying scheme and can be used to classify patterns into one of two categories (Example: Hail-no Hail, Tornado-no Tornado). The TLU works well if the patterns belonging to the two categories are linearly separable. A set of patterns in the n dimensional space (E_n) are linearly separable if there exists a hyperplane in E_n such that all the patterns belonging to one category lie on one side of the hyperplane. The equation of the hyperplane can be written as $g(\vec{X}) = \omega_1 X_1 + \omega_2 X_2 + \ldots + \omega_n X_n + \omega_{n+1} = 0$, where the "weights" $\omega_1, \omega_2 \ldots \omega_n, \omega_{n+1}$ are such that

$g(\vec{X}) > 0$ If $\vec{X}$ belongs to category I and

$g(\vec{X}) < 0$ If $\vec{X}$ belongs to category II.

$$\vec{X} = \begin{bmatrix} X_1 \\ X_2 \\ \cdot \\ \cdot \\ \cdot \\ X_n \end{bmatrix}$$

$g(X)$ is called the "discriminating function" and can be easily implemented according to Figure 15.

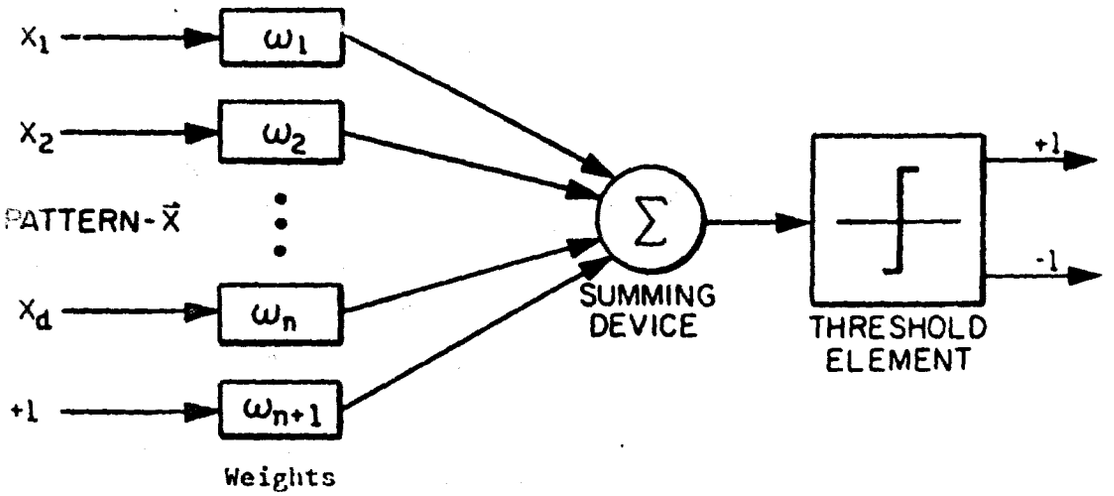

FIGURE 15. THRESHOLD LOGIC UNIT

The response of the threshold element is + 1 if $g(\vec{X}) > 0$, and is - 1 if $g(\vec{X}) < 0$. The pattern is classified as category I or II depending on whether the response is + 1 or - 1.

If one has a complete knowledge about all the patterns to be classified, then the weights $\omega_1, \omega_2, \ldots, \omega_{n+1}$ can be determined analytically. However, in most of the practical cases, only a few sample patterns are available. In such cases, these weights are determined by trial and error based on the sample patterns. The iterative method of arriving at the final values for the weights is called "training the TLU", and the patterns used in the process are referred to as the "training set." Training the TLU is done on a computer, and a computer

program has been written and checked out. For further description of TLU's see reference 2.

Nearest Neighbor Rule

The pattern classifying scheme based on the nearest neighbor rule is well suited for use in situations where the patterns belonging to a particular category tend to cluster. (Figure 16).

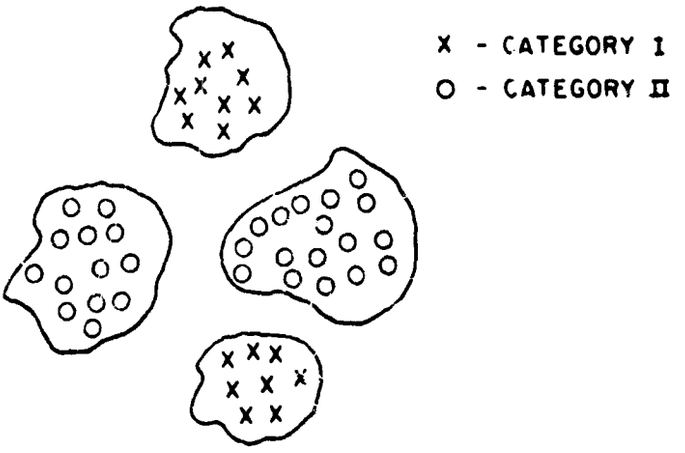

Figure 16. NEAREST NEIGHBOR RULE

As the name implies, the machine classifies the pattern $\vec{X}$ as coming from category j, if the training pattern nearest to $\vec{X}$ is of category j. A measure of nearness is the Euclidian distance given by

$$d(\vec{X}, \vec{P}_i^j) = \sqrt{(\vec{x} - \vec{p}_i^j) \cdot (\vec{X} - \vec{P}_j^j)}$$

where $d(\vec{X}, \vec{P}_i^j)$ is the distance between $\vec{X}$ and the i^{th} training pattern in the j^{th} category. The distance between $\vec{X}$ and the nearest pattern of j^{th} category is given by

$$d(j) = \min_i [d(\vec{X}, \vec{P}_i^j)] ,$$

and this is called D(j), the distance between X and the j^{th} category.

$\vec{X}$ is classified as category j if

$$D(j) < D(k), \quad k = 1, 2 \ldots R \; ; \; k \neq j$$

where R is the total number of categories.

For further description of nearest neighbor rules see reference 3. A computer program for nearest neighbor pattern classification has been written and checked out.

Data Reduction

Narrow Band Recording

The present set-up for digitising the analog data from the narrow band recording was outlined in the quarterly report dated June 30, 1968. On this set-up, the analog data is digitised using an EECO-761 A-D converter, and the digital samples are fed into the core memory of an IBM 1620 computer. After the core is filled, its contents are transferred to an IBM 1311 disk unit and stored there for further processing.

The analog to digital conversion is done on one track at a time, at the rate of 500 samples per second. In order to be able to look at identical sections of data on all the 12 tracks of data, a common time reference must be established. This time reference is established by masking the tape for a few inches. The masking produces zero analog output voltage on all the twelve channels, and this voltage appears as a string of zeros in the digital samples. This string of zeros can be easily identified and used as a time reference for locating sections of digital data on different channels corresponding to a particular interval of time.

Computer programs have been developed for further processing of the digital data from the narrow band recording. Programs are now in

use for calculating the average value of the signal, the amplitude distribution, and the sferic count, and the correlation between the signals in the horizontal and vertical channels for each frequency. At present, the digital data stored on IBM 1311 disks have to be transferred to punched cards before further processing can be done. This prevents a detailed analysis of large segments of narrow band data. However, new computing facilities are expected to be available at the end of fall 1968 (see section on data collection). This includes an IBM 360 computer which will accept input data directly from disk storage, thus eliminating the need for transferring the data to punched cards.

Wide Band Recording

The sampling rate required for analog to digital (A-D) conversion of the wide band recording is about 600,000 samples per second. The present A-D conversion equipment can handle a maximum rate of 500 samples per second. The wide band recording cannot be digitised at this rate without loosing much of the high frequency components of the signal. However, by expanding the time base of the wide band recording by a ratio of 1:1024, the effective sampling rate can be increased to 512,000 samples per second. At this sampling rate, it is possible to recover the components of the signal up to a frequency of 250 KHz.

A time base expansion of 1:1024 is obtained in two steps:

1. The original tape containing the recording taken at 60 ips is played back at a speed of 1 7/8 ips and recorded on a new tape at 60 ips. The new tape now has a time base expansion of 1:32.

2. The new tape when replayed at a speed of 1 7/8 ips expands the time base by another factor of 1:32, giving a total time base expansion of 1:1024 (32^2).

The digitising of wide band recording is in the final testing

stages. Programs have already been developed to Fast Fourier transform the digital data. Fast Fourier transforming is in effect an averaging; hence, it reduces the number of data points in the wide band data. Also, this gives a way of comparing the power spectrum so obtained with the narrow band mean square averaging.

The wide band recorder has a frequency response (± 3db) of 300-300,000 Hz at a recording speed of 60 ips. Hence, the signal coming off the wide band recording will have high frequency components up to and beyond 300 KHz. Because of the slower sampling rate of 512,000 per second, the power density spectrum of the signal obtained from these digital samples will have some error due to "aliasing." However an inspection of the narrow band (mean square averaged) recording of the signal indicates that the energy content is small at high frequencies beyond 250 KHz. Therefore, error due to aliasing can be neglected.

Measurement Selection

The digital samples obtained from the narrow band and wide band recordings constitute the data for the pattern recognition scheme. The narrow band comb filter outputs have been recorded continuously, while the wide band signal has been recorded for one minute duration once in every fifteen minutes. In order to be able to use the data from both the recordings to form pattern vectors, it is necessary to take segments of narrow band data for fifteen minutes duration and combine it with the corresponding wide band data for one minute duration. The combined data for this fifteen minute period is used to form one pattern vector.

At the ideal sampling rate, there are 36 million digital samples per minute from the wide band recording and about 360,000 samples per minute from the narrow band recording. It is not possible to use such

a large number of samples to describe patterns. Instead, a reasonable number of measurements (variables) characterising the data will be used to form the pattern vectors.

A set of 44 measurements have been chosen tentatively to describe the characteristics of the data taken over a period of fifteen minutes. Each of these variables is quantized into five levels, resulting in a maximum of 5^{44} distinct patterns. Quantizing is done to save memory storage on the computer and to increase the speed of computation. The nature of these measurements and their levels of quantizing are explained below.

Measurements From Wide Band Recording

Because of the large number of data samples, preprocessing is necessary on the wide band data before any measurements can be attempted. Fast Fourier transforming will be a preprocessing on wide band data, and a set of 14 measurements have been chosen to characterize the power density spectrum obtained by Fast Fourier transforming. These measurements describe the change in power density between two successive bursts of wide band recording at the following frequencies: DC (recovered from wide band F.M. recording), 10 KHz, 25 KHz, 50 KHz, . . . 300 KHz. The differences in power density, instead of the actual values, are taken because of two advantages:

1. By taking the difference in power density corresponding to two successive segments of data, some information about the past history of the signal is maintained.
2. Any bias or error in the measurements tend to cancel out.

Each of these 14 measurements are quantized into five levels as indicated below.

Amount of change in power density	Quantized value
Above 50% decrease compared to previous value	1

50-5% decrease compared to previous value 2

With in 5% of the previous value 3

5-50% increase over previous value 4

Above 50% increase over previous value 5

Measurements From Narrow Band Recording

A set of 30 measurements are taken to represent the characteristics of the data coming from the 12 channels of the narrow band recording. These measurements contain information about the sferic counts on each channel, the amplitude distribution, and the correlation between the signals in the horizontal and vertical channels.

Out os these 30 measurements, a set of 12 are chosen to measure the sferic counts on the 12 channels of data. The sferic count is taken with respect to a threshold level, which is set slightly higher than the average value of the signal in that channel.

$$V_T = V_A + \frac{(V_P - V_A)}{4}$$

V_A - Average value

V_P - Peak value

V_T - Threshold value

The sferic counts will be different on each channel, and the values of the sferic counts are quantized with respect to the average count over the 12 channels.

Actual Values of the Sferic Count	Quantized value
Less than 50% of the average value	1
Between 50-95% of the average value	2
Between 95-105% of the average value	3
Between 105-150% of the average value	4
Over 150% of the average value	5

Characteristics of the amplitude distribution of the data are

presented by a set of 12 measurements. Each measurement represents the percentage of total time during which the signal in a particular channel is above the threshold value set for that channel. The actual values of the measurements on the amplitude distribution are quantized as follows.

Actual value of time	Quantized value
Below 20%	1
Between 20-40%	2
Between 40-60%	3
Between 60-80%	4
Above 80%	5

Six measurements are taken to represent the correlation between signals in the horizontal and vertical channels at frequencies 10 KHz, 50 KHz, 100 KHz, 150 KHz, 200 KHz and 250 KHz. The actual values of correlation are quantized as follows:

Actual Values of Correlation	Quantized value
Below 0.2	1
Between 0.2 to 0.4	2
Between 0.4 to 0.6	3
Between 0.6 to 0.8	4
Above 0.8	5

At this stage, it is not known if these measurements will be adequate to transform the data into recognizable patterns. However, after the initial training of the pattern recognition scheme, new measurements will be added if necessary. Also, some measurements may be omitted if the weights on the TLU corresponding to these measur

ments are very small compared to others. For further discussion on measurement selection see reference 4.

An Intermediate Pattern Classification Test

As mentioned earlier in this section, two nonparametric methods of pattern recognition--threshold logic unit and nearest neighbor rule--will be used to classify severe weather patterns. Two major steps involved in implementing these pattern recognition shcemes are

1. Taking measurements from the data to form the training patterns.
2. Training the computer to learn to classify the patterns in the training set.

Computer programs have been developed for obtaining measurements from the data to form pattern vectors and to classify them using the two nonparametric methods. Attempts are now being made to classify lightning discharges into two categories (cloud to cloud or cloud to ground) using these programs. A brief outline of the procedure is given below.

The edge tracks of the narrow band recordings taken during some recent storms contain brief descriptions about the nature of the lightning discharges based on visual observation from the aircraft. This description includes such details as the nature of the discharge and if the discharge occurred close to the aircraft. By correlating with this information, any particular burst of activity in the narrow band channels can be identified as due to a cloud to cloud discharge or cloud to ground discharge. Sections of narrow band data corresponding to individual discharges have been digitised and plotted using an IBM 1620 computer and Calcomp plotter.

Figure 17 and 18 show the digital plots of the narrow band signal due to two cloud to cloud discharges. The signals in the horizontal and vertical channels at three frequencies (10 KHz, 50 KHz, and 150 KHz)

TOP - SIGNAL IN 10 Khz HORIZONTAL CHANNEL
BOTTOM - SIGNAL IN 10 Khz VERTICAL CHANNEL

TIME SCALE: 1" = 100 MILLISECONDS

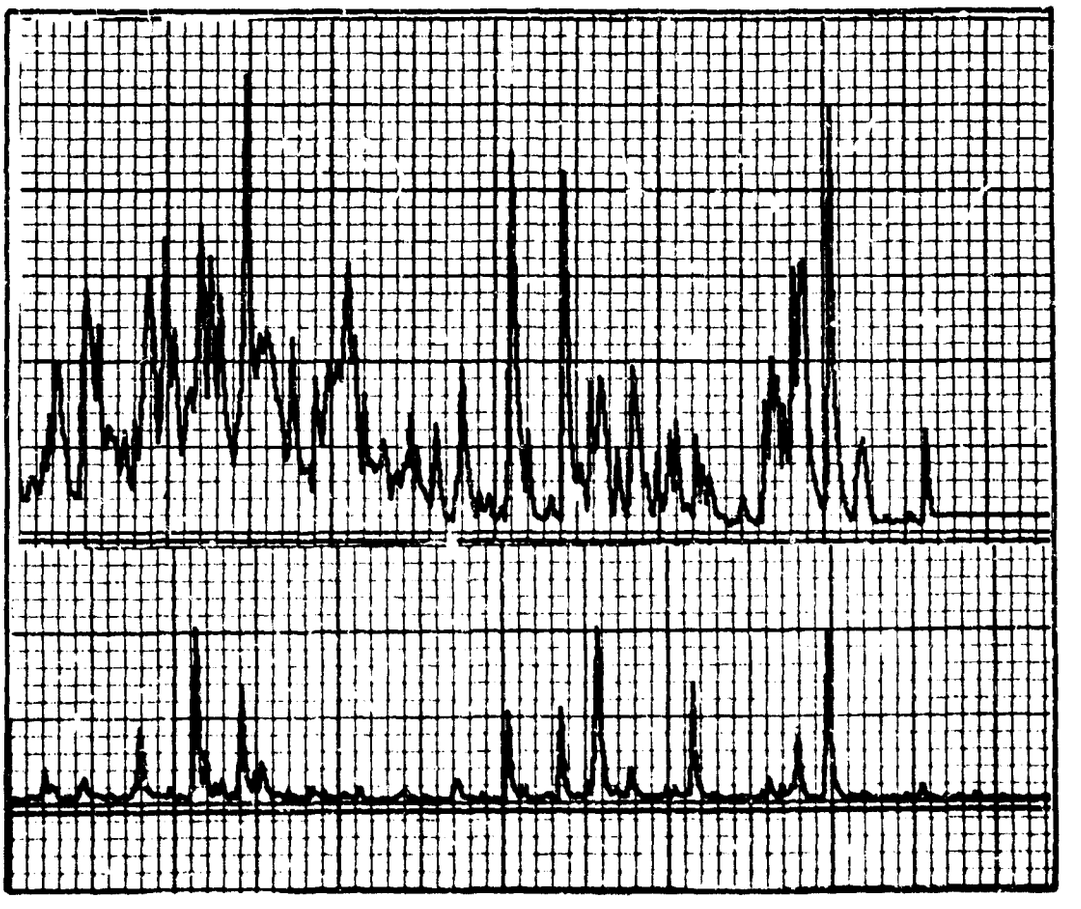

FIGURE 17a. CLOUD TO CLOUD DISCHARGE I.

TOP - SIGNAL IN 50 Khz HORIZONTAL CHANNEL
BOTTOM- SIGNAL IN 50 Khz VERTICAL CHANNEL

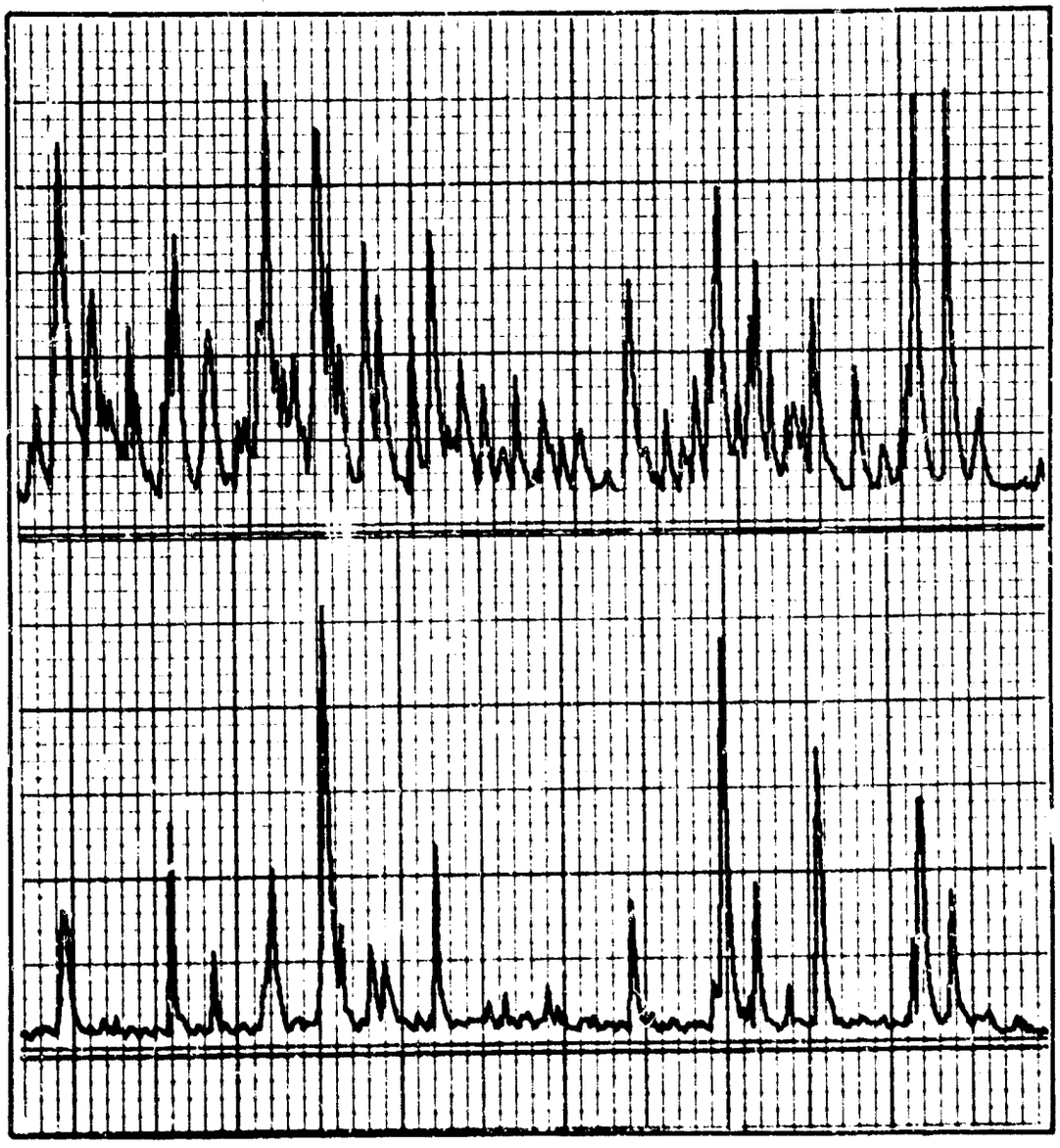

FIGURE 17b. CLOUD TO CLOUD DISCHARGE I.

TOP - SIGNAL IN 150 Khz HORIZONTAL CHANNEL
BOTTOM - SIGNAL IN 150 Khz VERTICAL CHANNEL

TIME SCALE: 1" = 100 MILLISECONDS

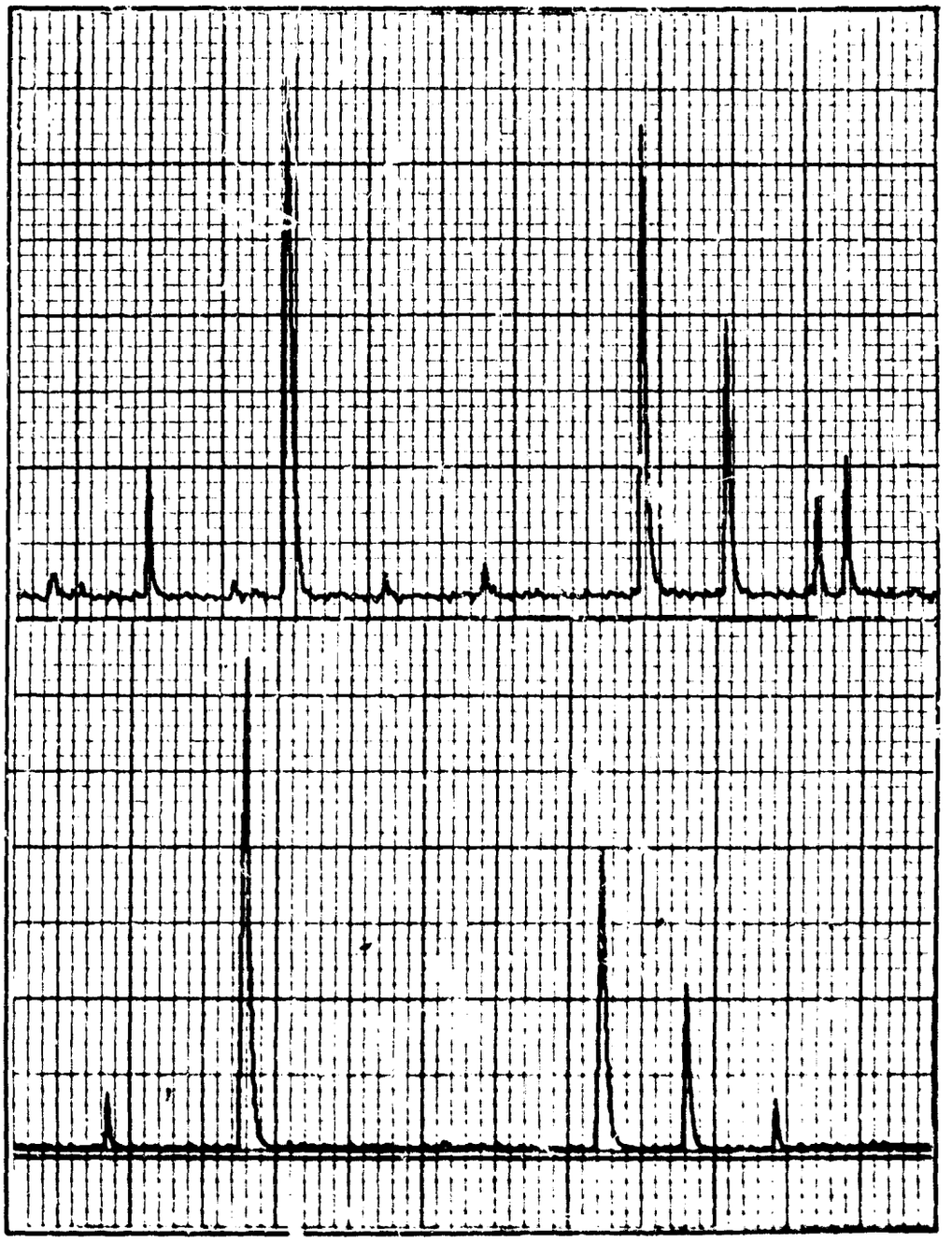

FIGURE 17c. CLOUD TO CLOUD DISCHARGE I

TOP - SIGNAL IN 10 Khz HORIZONTAL CHANNEL
BOTTOM - SIGNAL IN 10 Khz VERTICAL CHANNEL

TIME SCALE: 1" = 100 MILLISECONDS

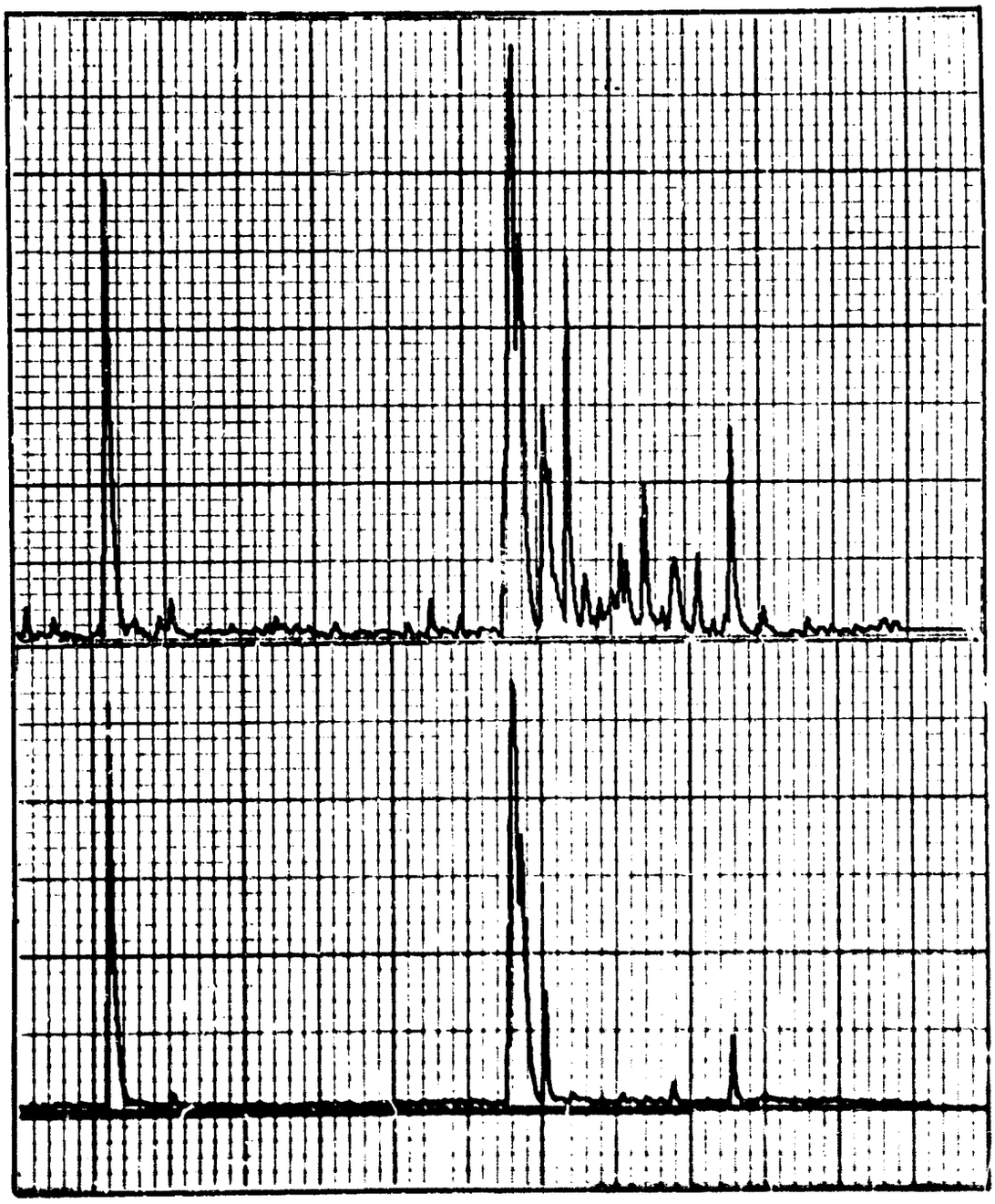

FIGURE 18a CLOUD TO CLOUD DISCHARGE II.

TOP - SIGNAL IN 50 Khz HORIZONTAL CHANNEL
BOTTOM - SIGNAL IN 50 Khz VERTICAL CHANNEL

TIME SCALE: 1" = 100 MILLISECONDS

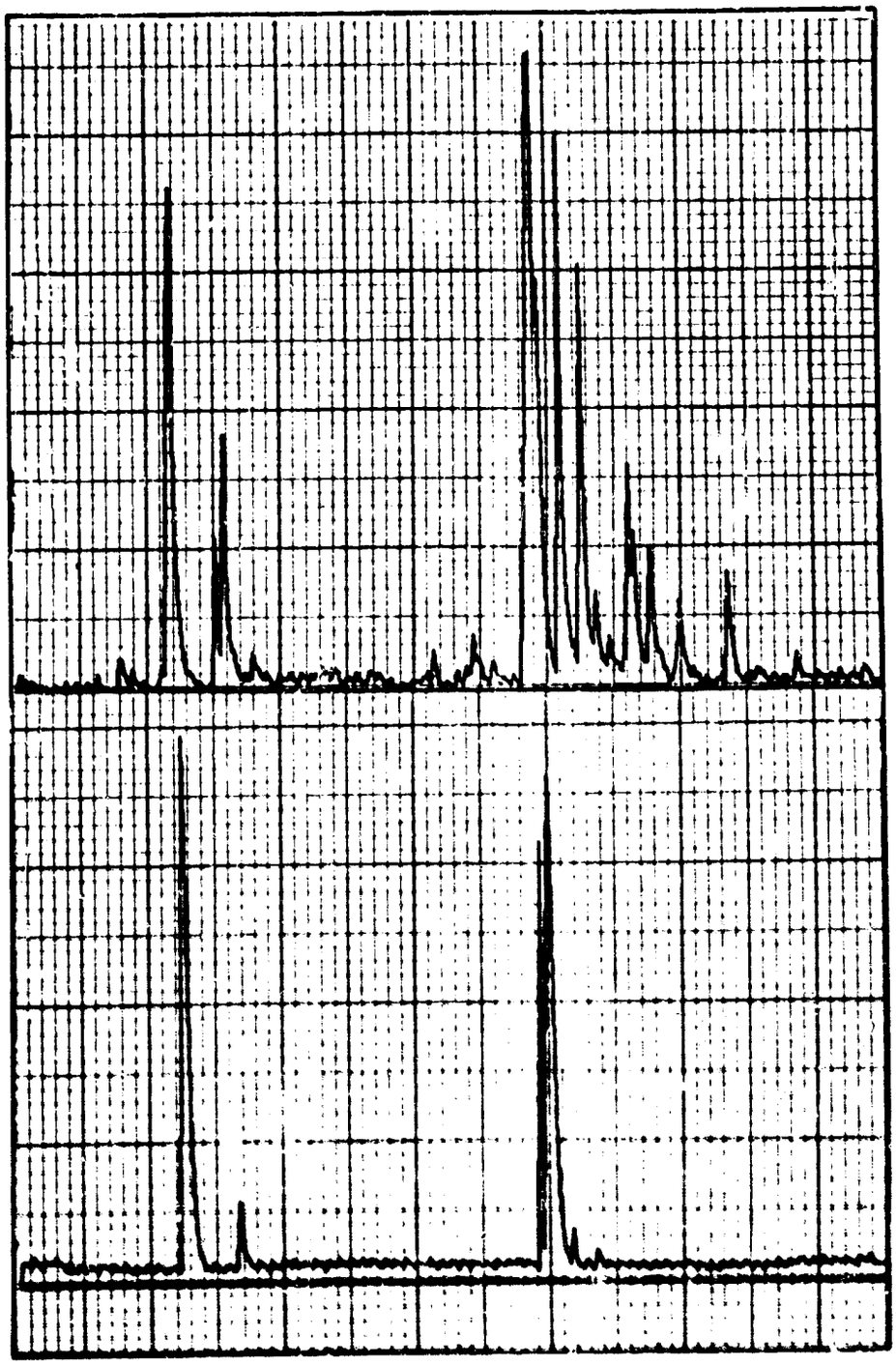

FIGURE 18b CLOUD TO CLOUD DISCHARGE II

TOP - SIGNAL IN 150 Khz, HORIZONTAL CHANNEL
BOTTOM - SIGNAL IN 150 Knz, VERTICAL CHANNEL

TIME SCALE: 1" = 100 MILLISECONDS

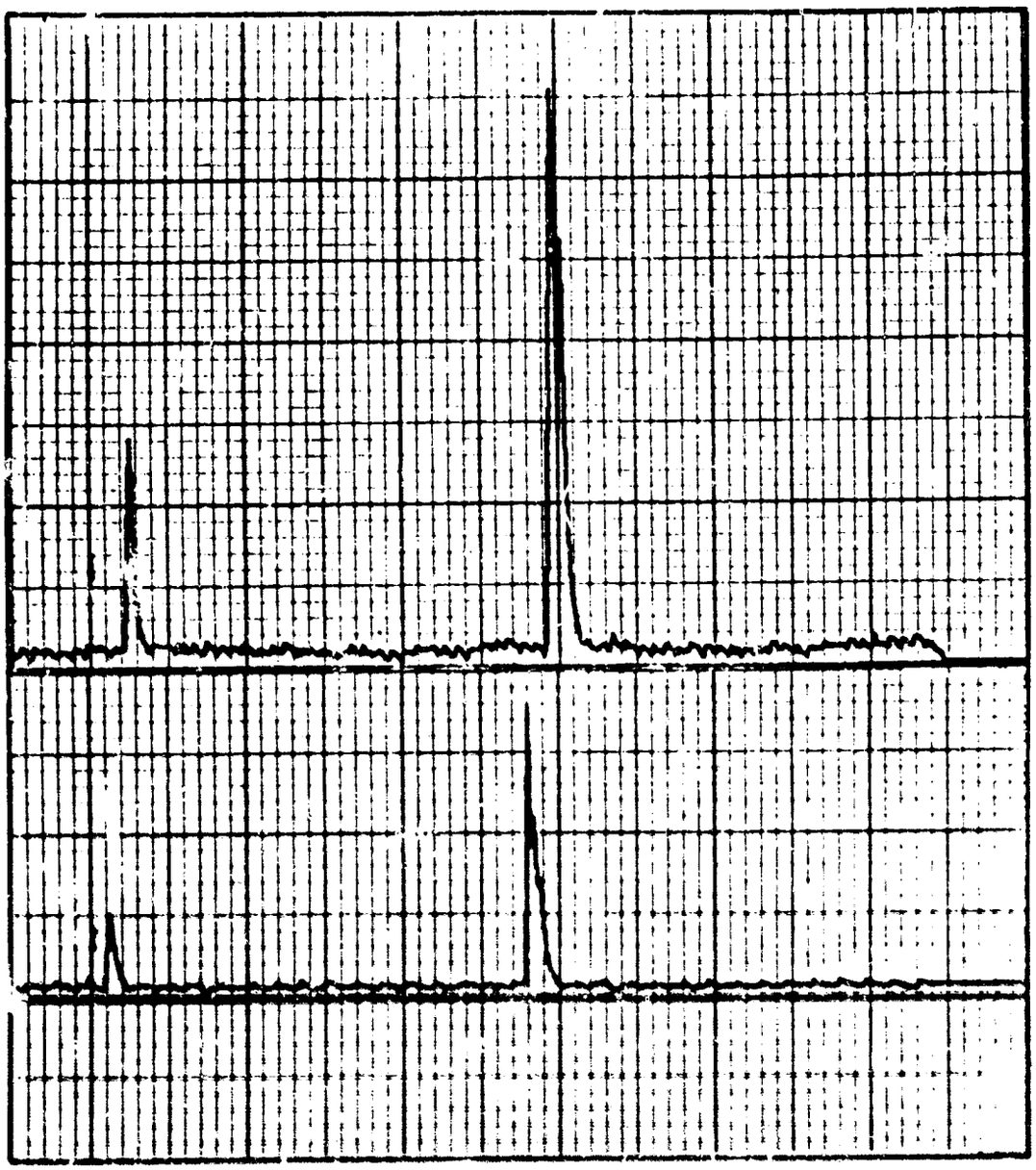

FIGURE 18c. CLOUD TO CLOUD DISCHARGE II.

are shown in these figures. Figure 19 shows the plot of a cloud to ground stroke. At each frequency the gain is the same for the horizontal and vertical channels. An inspection of these plots leads to the belief that there is more activity in the vertical channels during a cloud to ground discharge compared to a cloud to cloud discharge. (It is hoped that the computer will recognize this difference, through our measurements).

A set of 30 measurements taken from the narrow band data is used to form training patterns. This set of measurements is the same as the one outlined in section II-D (on measurement selection). Training patterns for each category are now being formed. Pattern recognition will be attempted after a reasonable number of training patterns have been obtained. Then the trained computer will be tested on other samples.

The data, the measurements, and the techniques used here to classify lightning discharges are similar to the ones that will be used later to classify severe weather patterns. Therefore, it is hoped that the experience gained through this intermediate attempt will be helpful when classifying meteorological phenomenon.

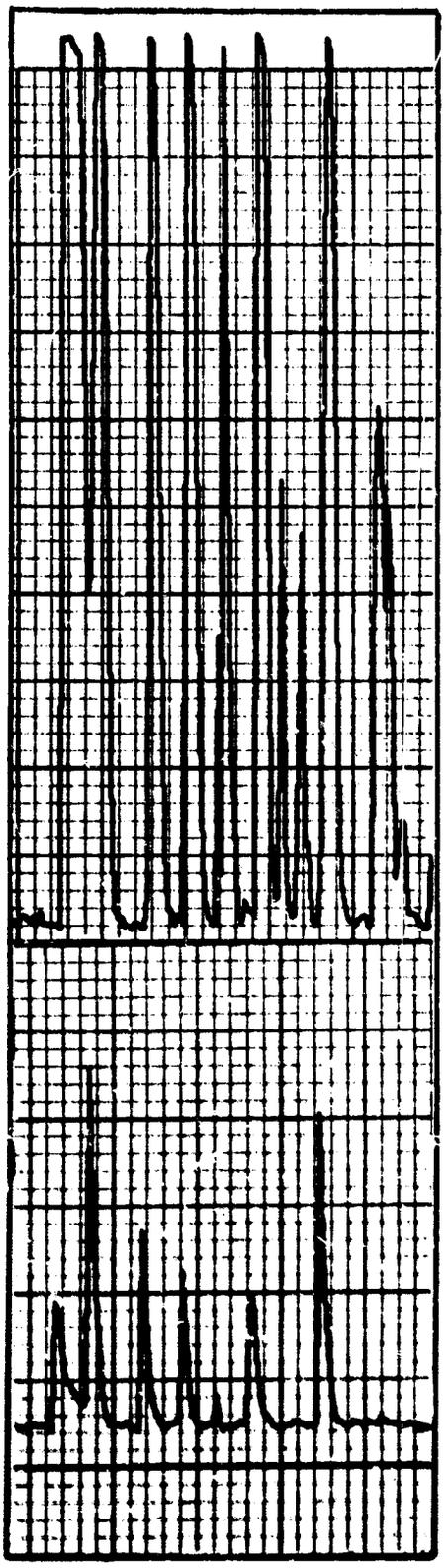

TOP - SIGNAL IN 10 Khz
HORIZONTAL CHANNEL

BOTTOM - SIGNAL IN 10 Khz
VERTICAL CHANNEL

TIME SCALE: 1" = 100 MILLISECOND

FIGURE 19a. CLOUD TO GROUND STROKE.

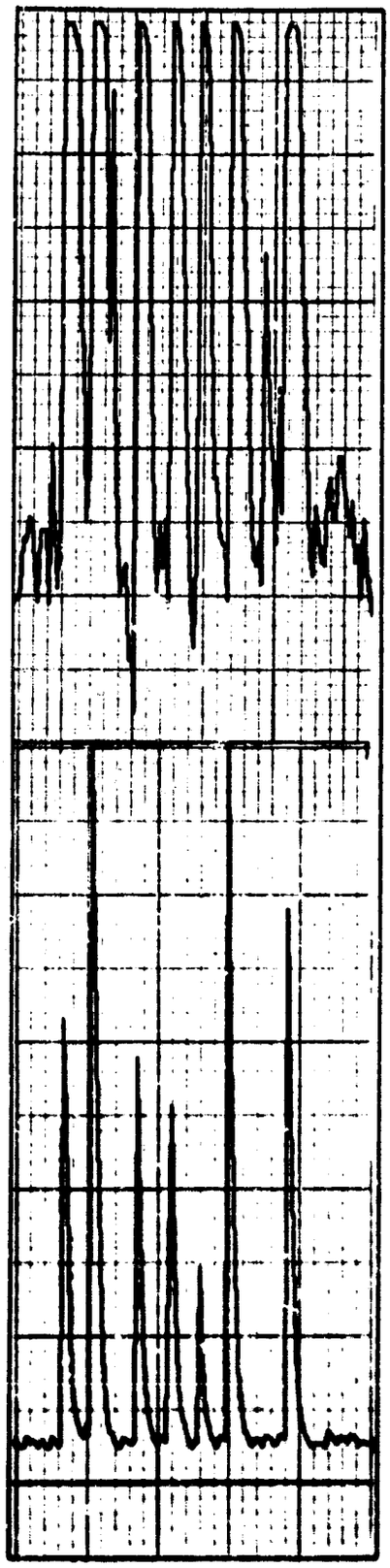

TOP - SIGNAL IN 50 Khz
HORIZONTAL CHANNEL

BOTTOM - SIGNAL IN 50 Khz
VERTICAL CHANNEL

TIME SCALE: 1" = 100 MILLISECONDS

FIGURE 19b. CLOUD TO GROUND STROKE.

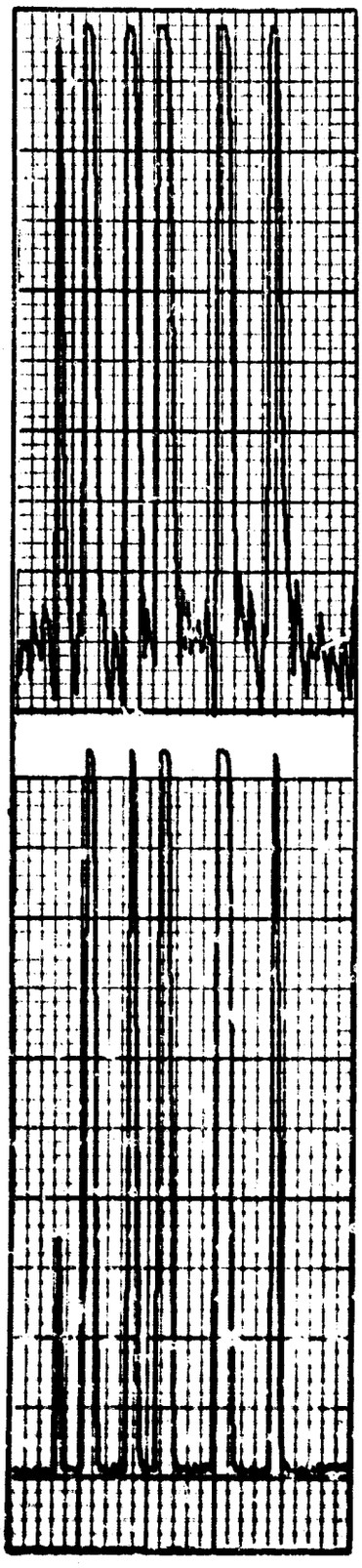

TOP - SIGNAL IN 150 Khz
HORIZONTAL CHANNEL

BOTTOM - SIGNAL IN 150 Khz
VERTICAL CHANNEL

TIME SCALE: 1" = 100 MILLISECONDS

FIGURE 19c. CLOUD TO GROUND STROKE.

V. DATA ANALYSIS

A. USE OF EXISTING FACILITIES

An IBM 7040 digital computer is presently available for processing data recorded in the aircraft. To date, the 7040 has been used primarily for program development and checkout; also, some preliminary runs have been made on actual atmospheric data.

Within the month, the 7040 machine will be replaced by an IBM 360/50 computer.

Before either of the computers can be used, the raw data, recorded on magnetic tape in analog form, must be digitized and put on a media acceptable as input to the digital computer. In addition, the higher frequency data must be "time-scaled" by slowing down the tape machine speed on playback.

Selected portions of low-frequency data are presently being digitized and the results punched into cards through the use of an existing slow-speed system. This system is extremely inadequate as far as the preparation and storage of long runs and many runs of data are concerned; however, it is serving to furnish realistic data for the testing of the various programs.

Briefly, the characteristics and details of operation of the system are shown in Figure 20. The data tape is played back at the ground laboratory, and the signal is conditioned in a preamp to a standard range of 0-5 volts. The signal is then fed into an analog to digital converter which converts the samples to BCD digital form. Each sample consists of three decimal digits.

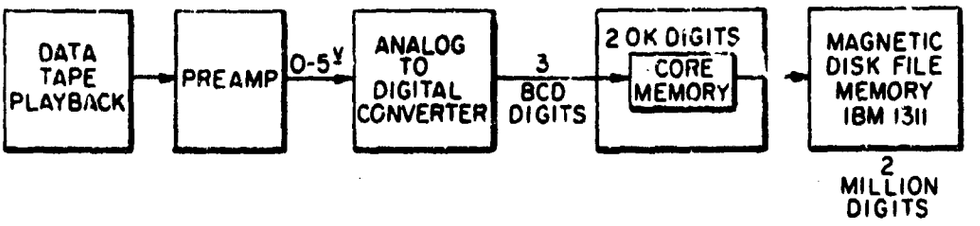

MAX Sample rate = 500 Samples/sec
MAX Duration of one sample run = 6 sec
TIME Required to dump core to disk = 1/20 sec

Figure 20. PRESENT DIGITAL DATA PREPARATION EQUIPMENT

The sampling process continues until the core memory of the 1620 computer, shown in Figure 20, is effectively filled. The computer then dumps its core memory and then proceeds to resume the sampling process.

The speed and volume handling capabilities of the system are primarily limited by the speed and core memory size of the 1620 computer. The system can convert data at a maximum rate of 500 samples per second for an uninterrupted duration of 3000 samples. At this time, the core memory must be dumped into the disk, and this requires approximately 0.05 second.

Later, the data on the disk is punched into cards, 20 samples per card. Obviously, the digitizing of even a moderate amount of data results in an exorbitant number of cards.

New Equipment

In order to seriously pursue the preparation of the data obtained from the flight recorders, new equipment must be secured. In brief, this is because sampling rates must go as high as 20,000 samples per

second for extended runs involving up to approximately 2 million samples. So, not only must this supporting equipment possess a much higher speed capability than the existing equipment, but it also must have a much larger and higher density storage media. This dictates digital magnetic tape as the output storage media of the system; and, the form of the digitized data on this tape must be compatible with the IBM 360/50 computing system.

Furthermore, since the 360/50 system will not have a graphical plotting feature, it is virtually imperative that any proposed new equipment should include this capability. A Calcomp plotter is presently available, so the equipment will only need the necessary interfacing and control.

Some of the recorded flight data represents analog atmospheric energy with information frequencies as high as 250 kilohertz, approximately. The tape with this data can be slowed down by a ratio of 32 to 1 upon playback, thus effectively frequency scaling the data by the same ratio. The scaled data can then be said to contain frequencies of up to $250/32 \tilde{=} 8$ KHz.

In order to adequately represent this scaled data in digital form, a minimum sampling rate of approximately 20,000 samples per second is dictated.

A typical burst of atmospheric signal will require a total number of samples in the range of 1 to 2 million without any gaps in the data vector in order to make possible the desired analysis procedures.

A number of digital conversion systems have been investigated and quotations were obtained on several. The system that combines an acceptable cost with the desired specifications of sample speed, tape input, tape output (9 channel, IBM), plotter interface, and a flexible method of data editing control, is the Hewlett-Packard 2115A system equipped with an HP3030 tape machine and an EEC0761A analog to digital converter.

Steps have already been initiated to purchase this system; once the order is received by the Hewlett-Packard Company, delivery is expected to be 12-14 weeks.

In summary, the new system being proposed will accept analog data and digitize it at rates of up to at least 20,000 samples per second. The output will be put on a nine-track magnetic tape in a form compatable with the IBM 360/50 system. This sampling task can continue until the output tape is filled. The output tape will accommodate approximately 10 million samples if desired.

Output from the analysis programs (also on nine-track magnetic tape) run on the 360/50 computer can be read into the HP2115A system and plotted on a Calcomp plotter.

B. DIGITAL DATA REDUCTION AND TRANSFORMATION

The exact data reduction and analysis processes to be applied to the collected data are, as yet, not known. However, it seems that Fourier Analysis will undoubtedly be of primary interest in study of the wide-band signal recordings. With the wide-band analog data sampled and recorded in digital form (suitable for direct input to the University's IBM 360/50 computer), the Finite Discrete Fourier Transform is applicable for such analysis. The Cooley-Tukey algorithm [5] provides an efficient high-speed implementation for the necessary processing.

However, because of the large bandwidth of the signal (0-250 KHz), meaningful analysis of data-tracks only one or two seconds length will involve large streams of data. Samples of one or two million observations may, on occasion, be of interest. The direct, in-core manipulation of such large data-vectors is not possible in the available digital computer. Therefore, development of a computer program (in Fortran IV) has been carried out to perform the Fast Fourier Transform (FFT) on large data-vectors.

A highly-efficient program for performing the FFT on in-core data-vectors is available from the SHARE library [6]. This program is used as the nucleus for the large-vector program which has been developed. As outlined by Gentleman and Sande [7] and Singelton [8], the FFT can be performed on subsections of a large data-vector by a series of pre-transform operations on the segments. The number of such pre-transfrom phases is dependent on the number of subsections required -- each subsection finally being submitted to the FFT program in-core.

For example, suppose that the largest data-segment that can be handled in-core with the FFT program is 4096 samples. A data-vector of 65,536 samples can be handled in 16 subsections. This would require four pre-transform phases ($s^4=16$) followed by submission of each of the 16 subsections to the FFT program.

Following the 16 FFT operations, a number of post-sorting phases are required (again 4 for the example 16 sections) to re-order the data into proper sequence. The program to implement this has been thoroughly tested on the existing computer facility, an IBM 7040. The pre-transform and post-sorting is accomplished using four scratch tapes for temporary storage.

The 360/50 installation is due for activation in early November, and will have available the IBM 2314 Disk Storage Facility (8 cordinated 11-disk storage units). It is planned to begin immediate program modification to utilize the disk storage faciltiy for the pre-transform and post-sort operations. With 256kB of core storage available and the overlap of I/O and CPU functions, it is anticipated that an appreciable improvement in total execution time can be obtained. The program structure places no upper limit on the data-vector size -- the increase of execution time for very large vectors will determine the allowable sample size.

If the Fourier Analysis of digitized data is eventually determined to be of critical importance, and the required execution-time is a limiting factor, a number of alternatives are available. Hardware implementation of the Fast Fourier Transform by array-processor techniques offers great promise. A vector of 1024 samples can be

transformed by such "black-boxes" in times of the order of 40 milliseconds. The time increases in the order of N $\log_2 N$, where N is the sample size. These "black-boxes"are currently available for direct addition to the IBM 360 machines in the form of an additional I/O channel. They operate in the "cycle-stealing" mode, and allow normal CPU operation once they are commanded to operate. Coupled with graphics-display devices, they offer the promise of "almost real-time" Fourier Analysis and spectral display for quite large data-samples.

VI. CLOUD MODELING

A preliminary study of the basic hydrodynamic equations of two-dimensional vortex flow as they apply to an idealized tornado funnel was made in order to ascertain whether a highly restricted mathematical model would produce reasonably accurate predictions. The results obtained indicate that this preliminary effort was successful.

The results of the tornado investigation are shown on the following pages of this section.

References 9 through 14, Appendix A, were used in the investigation of the idealized tornado funnel.

A. ASSUMPTIONS

1. The tornado energy is supplied by water condensation in the funnel.
2. The rising heated air in the funnel is equivalent to a vertical-cone-sink for the inward spiralling air.
3. The radial and tangential air velocities do not depend on time, and depend only weakly on height.
4. The air outside the funnel is approximately incompressible.
5. The heating of the air by its own sheer-friction is negligible.

B. GENERAL EQUATIONS

1. Navier-Stokes Equations

$$\nabla \cdot (\rho V) + \frac{\partial \rho}{\partial t} = 0$$

$$\frac{\partial V}{\partial t} + (V \cdot \nabla) V = \frac{-\nabla(p+q)}{\rho} + \frac{\mu}{3\rho} \nabla(\nabla \cdot V) + \frac{\mu}{\rho} \nabla^2 V$$

t = time (sec)

ρ = local fluid density ($gm\ cm^{-3}$)

μ = fluid viscosity ($dyne\ sec\ cm^{-2}$)

V = fluid velocity vector ($cm\ sec^{-1}$)

q = external field-potential (erg cm^{-3})

$$(V\cdot\nabla)V = \nabla(V\cdot V)/2 - V\times(\nabla\times V)$$

$$\nabla^2 V = \nabla(\nabla\cdot V) - \nabla\times(\nabla\times V)$$

∇, $\nabla\cdot$, $\nabla\times$ = gradient, divergence, curl

2. Specialized Equations

q = 0, steady state, ρ = constant

No vertical component in V

$\hat{j}_r$, $\hat{j}_\theta$ = unit radial and tangential vectors

$$V = \hat{j}_r\, u(r) + \hat{j}_\theta\, v(r)$$

$$\rho(V\cdot\nabla)V + \nabla p = \mu\nabla^2 V$$

$$\nabla\cdot V = 0$$

$$u(a) = -s \quad , \quad v(a) = w$$

C. EQUATION REDUCTIONS

$$\frac{\partial u}{\partial\theta} = \frac{\partial u}{\partial z} = \frac{\partial v}{\partial z} = \frac{\partial v}{\partial\theta} = \frac{\partial u}{\partial t} = \frac{\partial v}{\partial t} = 0$$

$$\nabla\cdot V = 0 \rightarrow \frac{1}{r}\frac{\partial}{\partial r}(ru) + \frac{1}{r}\frac{\partial v}{\partial\theta} = 0$$

$$ru = \text{constant} = -as \qquad (1)$$

$$[(V\cdot\nabla)V]_r = u\frac{\partial u}{\partial r} - \frac{v^2}{r} \qquad [\nabla^2 V]_r = \frac{1}{r}\frac{\partial}{\partial r}\left(r\frac{\partial u}{\partial r}\right) - \frac{u}{r^2}$$

$$[(V\cdot\nabla)V]_\theta = u\frac{\partial v}{\partial r} + \frac{uv}{r} \qquad [\nabla^2 V]_\theta = \frac{1}{r}\frac{\partial}{\partial r}\left(r\frac{\partial v}{\partial r}\right) - \frac{v}{r^2}$$

$$\frac{\partial p}{\partial r} = \mu\left[\frac{1}{r}\frac{\partial}{\partial r}\left(r\frac{\partial u}{\partial r}\right) - \frac{u}{r^2}\right] - \rho\left[u\frac{\partial u}{\partial r} - \frac{v^2}{r}\right] \qquad (2)$$

$$0 = \mu\left[\frac{1}{r}\frac{\partial}{\partial r}\left(r\frac{\partial v}{\partial r}\right) - \frac{v}{r^2}\right] - \rho\left[u\frac{\partial v}{\partial r} + \frac{uv}{r}\right] \qquad (3)$$

$$\frac{1}{r}\frac{\partial}{\partial r}\left(r\frac{\partial u}{\partial r}\right) - \frac{u}{r^2} = \frac{1}{r}\frac{\partial}{\partial r}\left(\frac{as}{r}\right) + \frac{as}{r^3} = 0$$

$$u\frac{\partial u}{\partial r} - \frac{v^2}{r} = \left(\frac{-as}{r}\right)\left(\frac{as}{r^2}\right) - \frac{v^2}{r} = \frac{-1}{r}\left[v^2 + \left(\frac{a}{r}\right)^2 s^2\right]$$

$$u\frac{\partial v}{\partial r} + \frac{uv}{r} = \left(\frac{-as}{r}\right)\frac{\partial v}{\partial r} + \left(\frac{-as}{r}\right)\frac{v}{r} = (-as)\left[\frac{1}{r}\frac{\partial v}{\partial r} + \frac{v}{r^2}\right]$$

$$\left(\frac{\partial^2 v}{\partial r^2} + \frac{1}{r}\frac{\partial v}{\partial r} - \frac{v}{r^2}\right) + \frac{\rho}{\mu}\frac{as}{r}\left(\frac{\partial v}{\partial r} + \frac{v}{r}\right) = 0 \qquad (4)$$

$$\frac{\partial p}{\partial r} = \frac{\rho}{r}\left[v^2 + \left(\frac{a}{r}\right)^2 s^2\right] \qquad (5)$$

D. TANGENTIAL VELOCITY EQUATION

$$k = \frac{as}{\mu/\rho}$$

$$r^2\frac{\partial^2 v}{\partial r^2} + (1 + k)\, r\frac{\partial v}{\partial r} - (1 - k)v = 0$$

Note: According to Sinclair's work on dust devils, μ/ρ = 5-15 $m^2\ sec^{-1}$.

Limiting case of infinite viscosity

$$\mu \to \infty \text{ means } k \to 0$$

$$\frac{\partial^2 v}{\partial r^2} + \frac{1}{r}\frac{\partial v}{\partial r} - \frac{v}{r^2} = 0 \quad \frac{\partial}{\partial r}\left[\frac{1}{r}\frac{\partial}{\partial r}(rv)\right]$$

This is satisfied by the equation

v = ωr of a rotating solid.

Limiting case of zero viscosity

$$\mu \to 0 \quad \text{means} \quad k \to \infty$$

$$r \frac{\partial v}{\partial r} + v = 0 = \frac{\partial}{\partial r}(rv)$$

This is satisfied by the equation

$v = aw/r$ of a perfect vortex.

Limiting case of crucial sink (k = 1)

$$r^2 \frac{\partial^2 v}{\partial r^2} + 2r \frac{\partial v}{\partial r} = 0 = \frac{}{r}(r^2 \frac{\partial v}{\partial r})$$

This is satisfied by the equation

$v = w - c[1 - (a/r)]$ where w and c are constants.

E. EQUATION SOLUTION

$$r^2 \frac{\partial^2 v}{\partial r^2} + (1 + k)r \frac{\partial v}{\partial r} - (1 - k)v = 0$$

$$\lim_{r \to a} [v] = w , \qquad \lim_{r \to \infty} [v] = 0$$

Use of the substitution $r = ae^{\alpha}$ gives

$$\frac{\partial^2 v}{\partial \alpha^2} + k \frac{\partial v}{\partial \alpha} - (1 - k)v = 0$$

$$\lim_{\alpha \to 0} [v] = w , \qquad \lim_{\nabla \to \infty} [v] = 0 ,$$

which has the standard-form solution

$$v = Ae^{-\alpha} + B\alpha^{-(k - 1)\alpha}$$

$$A + B = w , \qquad k > 1 ,$$

which in terms of the original radial coordinate r becomes

$$v = A \cdot (\frac{a}{r}) \cdot B \cdot (\frac{a}{r})^{k-1}$$

$$A + B = w , \qquad k > 1 .$$

F. RAOTATIONAL KINETIC ENERGY

Let h be the vertical thickness of a disk-shaped slice made through the tornado parallel to the ground, and let E be the rotational kinetic energy of this slice extending radially from r = a to r = ∞.

$$E = \int_a^\infty \frac{\rho v^2}{2} \cdot 2\pi r h \cdot dr = \pi\rho h \int_a^\infty r v^2 dr$$

$$= \pi\rho h \int_a^\infty r \cdot \left[\frac{Aa^2}{r^2} + \frac{2ABa^k}{r^k} + \frac{B^2 a^{2k-2}}{r^{2k-2}}\right] dr$$

$$= \pi\rho h \left[Aa^2 \operatorname{Ln} r + \frac{2ABa^k}{2-k} r^{2-k} + \frac{B^2 a^{2k-2}}{4-2} r^{4-2k}\right]_a^\infty$$

It is apparent from the result that E will be finite if and only if A = 0 and k > 2. Consequently,

$$E = \frac{\pi\rho h B^2 a^2}{2k-4} = \frac{\pi a^2 h \rho w^2}{2(k-2)}$$

$$k > 2 \quad , \qquad v = w \cdot \left(\frac{a}{r}\right)^{k-1} .$$

G. ANGULAR MOMENTUM

$$J = \int_a^\infty \rho r v \cdot 2\pi r h \cdot dr = 2\pi\rho h \int_a^\infty r^2 v dr$$

$$= 2\pi\rho h \int_a^\infty w a^{k-1} \cdot r^2 \cdot r^{1-k} \cdot dr$$

$$= 2\pi\rho h\, w a^{k-1} \cdot \left[\frac{r^{4-k}}{4-k}\right]_a^\infty$$

It is apparent from this result that J will be finite if and only if k > 4. Consequently,

$$J = \frac{2\pi\rho h a^3 w}{k-4} \quad , \quad k > 4 \quad .$$

H. GRAPHICAL RESULTS

The following page (Figure 21) shows in graphical form the circling wind speed outside a tornado funnel, calculated from the tangential velocity formula for $k = 4$, $k = 6$, and $k = 8$. Since the angular momentum of the tornado is finite only if $k > 4$, it is seen that in all admissible cases the circling wind speed falls to less than ten percent of its funnel-wall value beyond a distance of three funnel radii.

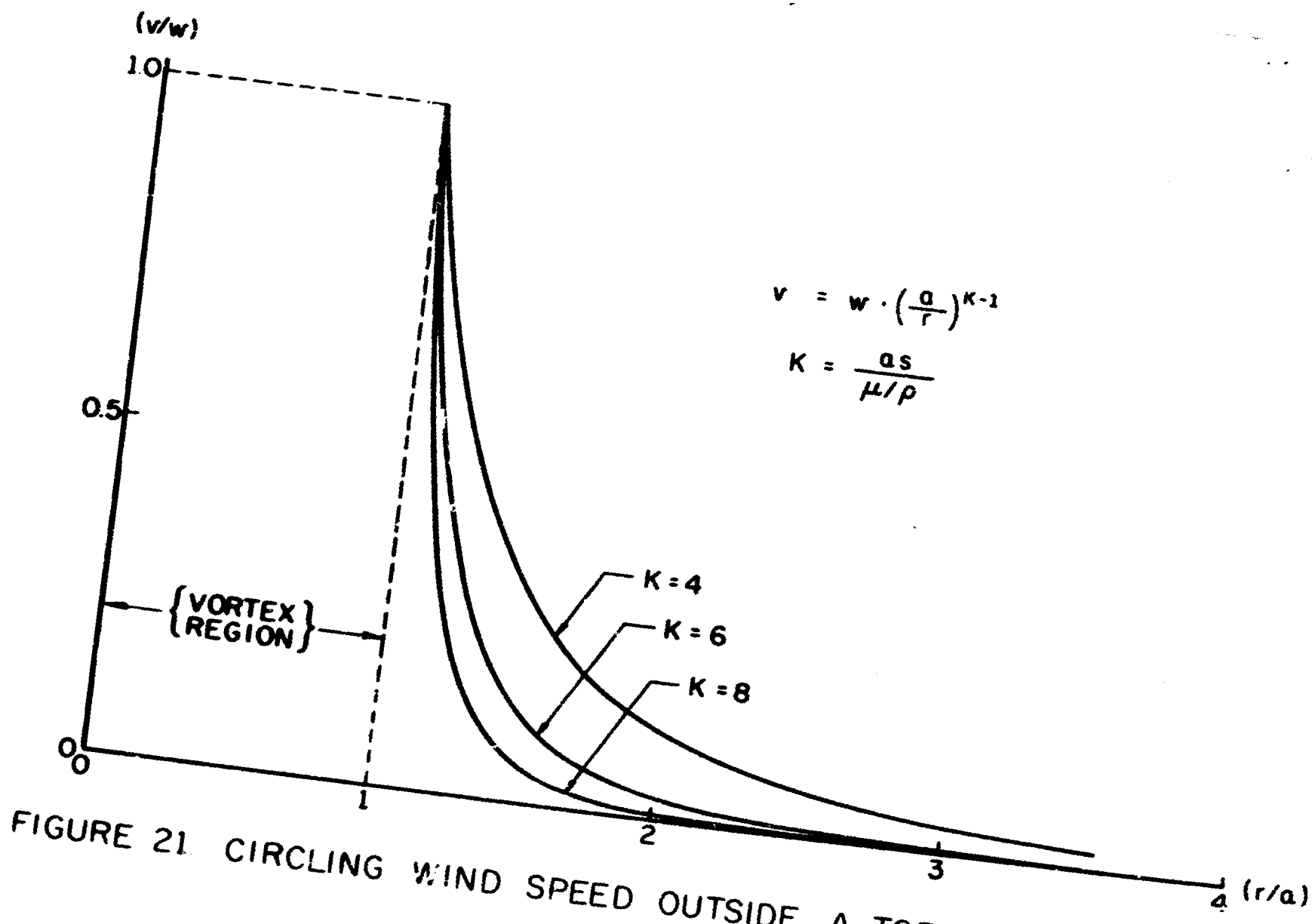

$$v = w \cdot \left(\frac{a}{r}\right)^{K-1}$$

$$K = \frac{as}{\mu/\rho}$$

FIGURE 21 CIRCLING WIND SPEED OUTSIDE A TORNADO FUNNEL

I. CONCLUSIONS

The exact mathematical equations for the three-dimensional viscous and compressible air flow in the proximity of a tornado funnel are extremely complex, and require a large investment of further analytical and computer effort in order to develop fully adequate solutions. The preliminary analysis presented here deals only with two-dimensional laminar and incompressible flow in a thick disk aligned co-axially with the funnel axis.

A rather peculiar formula for the tangential air velocity resulted from the solution of the equations of the restricted system. The circling wind speed was shown to decrease inversely with the (k - 1) power of the distance from the funnel axis, where k is a rather unique dimensionless constant. The denominator of the dimensionless ratio k is equal to the kinematic viscosity μ/ρ of the air, and the numerator is equal to the algebraic product of the funnel radius and the radial speed of air flow into the funnel. It was found that rotational kinetic energy of the spinning air disk cannot be finite unless $k > 2$, and that the angular momentum of the spinning diks cannot be finite unless $k > 4$. The constraint that $k > 4$ requires that the circling wind speed must decrease very rapidly with distance from the tornado funnel wall.

Inspection of photographs made of actual tornados indicates that the assumption of laminar flow is probably not a serious restriction except in the small region where the tornado funnel touches the ground. The assumption of incompressibility is more serious in the vicinity of the tornado wall, where the circling wind speed is frequently said to approach half the speed of sound.

The more elaborate study should concentrate first on the removal of

the incompressibility restriction and then take into account the vertical component of air flow as influenced by gravity and the equation of continuity.

APPENDIX A

REFERENCES CITED

REFERENCES CITED

1. Kraus, John D., Antennas, McGraw-Hill Book Company, Inc., 1950, p. 6.

2. Nils, J. Nilsson, Learning Machines, McGraw-Hill Book Company, Inc., 1965.

3. Highleyman, W. H., "Linear Decision Functions with Applications to Pattern Recognition," Proc. IRE, Vol. 50, No. 6, pp. 1501-1514, June, 1960.

4. Allais, D. C., "The Problem of Too Many Measurements in Pattern Recognition and Prediction," Rept. SEL-64-115, Stanford Electronics Laboratories, Stanford, California, November, 1964.

5. Cooley, J. W. and Tukey, J.W., "An Algorithm for the Machine Calculation of Complex Fourier Series," Mathematics of Computation, Vol. 19, No. 90, (1965) pp. 297-301.

6. SHARE program PX FRXM, "Finite Discrete Fourier Transform by the Cooley-Tukey Algorithm," Langdon and Sande, Princeton University, November, 1965.

7. Gentleman, W. M. and Sande, G. "Fast Fourier Transforms -- For Fun and Profit," Proceedings -- Fall Joint Computer Conference, 1966, Vol. 29, p. 569, Spartan Books.

8. Singeton, R. C., "A Method for Computing the Fast Fourier Transform with Auxiliary Memory and Limited High-Speed Storage," IEEE Transactions on Audio and Electroacoustics, June, 1967, Vol. AU-15, No. 2, pp. 91-97.

9. Sommerfeld, Arnold, Mechanics of Deformable Bodies, Academic Press, New York, 1964, pp. 77, 85, 113, 346-347.

10. Brodkey, Robert S., The Phenomena of Fluid Motions, Addison-Wesley Publishing Co., Reading, Mass., 1967, pp. 41-50.

11. Sinclair, Peter C., "A Quantitative Analysis of the Dust Devil," Ph.D. Thesis, University of Arizona, Tucson, Arizona, 1966, p. 229.

12. Korn, Granino A. and Korn, Teresa M., Mathematical Handbook for Scientists and Engineers, McGraw-Hill Book Company, New York, 1961, p.175.

13. Prandtl, L. and Tietjens, O. G., Fundamentals of Hydro and Aeromechanics, Dover Publications, New York, 1934 and 1957. pp. 251-250.

14. Li, Wen-Hsuing and Lam, San Hai, Principles of Fluid Mechanics, Addison-Wesley Publishing Company, Reading, Mass., 1964, p. 221.